

Geophilosophical Realness of Risk: A Case Study In National Housing Authority Resettlement Sites In Albay, Philippines

Ana Marie Rico Abante (✉ anamarie.abante@bicol-u.edu.ph)

Research

Keywords: geophilosophy, hotspots, coldspots, hexagonal bin, risk quantity, risk realness

Posted Date: August 7th, 2020

DOI: <https://doi.org/10.21203/rs.3.rs-52303/v1>

License: © ⓘ This work is licensed under a Creative Commons Attribution 4.0 International License.

[Read Full License](#)

Version of Record: A version of this preprint was published at SN Applied Sciences on March 24th, 2021.

See the published version at <https://doi.org/10.1007/s42452-021-04442-6>.

1 **GEOPHILOSOPHICAL REALNESS OF RISK:**
2 **A Case Study in National Housing Authority Resettlement Sites in Albay, Philippines**
3
4

5 Ana Marie R. Abante
6 anamarie.abante@bicol-u.edu.ph
7

8 **Abstract.** The *Geophilosophical* realness of risk, as introduced in this study constitutes risk **hotspots** or **coldspots** information
9 that are stored and sorted in **hexagonal bins** which represent geographical space. Using the binning technique, the author
10 disclosed the 29,400 hectares in Albay Philippines are 99% significantly sited as risk hotspot physical space. Also, about 7,100
11 hectares, and 3,100 hectares have 95% and 90% significant risk hotspots, respectively. This study also presents resiliency being
12 measured as a **risk quantity**, nearing a zero z-score that is enveloped by the fundamental geoinformation prerequisite to select
13 safe, comfortable, and accessible space. The z-scores represent the risk hotspots and coldspots contained in hexagonal bins which
14 mimic geographical aspects of the **risk realness** in Albay. The same z-scores were substituted for the 25 resettlement sites which
15 provided answers to the query “what are the risk realities in NHA resettlement sites?” The results characterized the risk that are
16 spreading at 14 resettlement’s sites in Albay are generally located within risk hotspot areas. This information is significant in
17 preventing and mitigating risk receptively and responsively. The researcher concludes that DRRM entails interdisciplinary
18 thinking to apply geospatial data science to risk governance. This dissertation revealed that government intervention may be
19 ineffective when people are steadily allowed to occupy risk hotspots that weakens their capacity to defy the quantified risk as
20 well as the accumulated and unbearable risk residuals caused by the unforeseen effects of changing climate such as volcanic
21 eruptions, lahar, increasing flooding, and pandemics. The *Metatheorems* in this study posit that dependable preparedness is
22 unlikely if the risk hotspots and coldspots of geographical locations are unknown or unclear, which would guide environmental
23 planners, engineers, development managers, and decision makers to direct the people to suitably select safe space, comfortable
24 sites, and accessible sites. Furthermore, this study presents that scientifically informed policy is a must-risk-reduction solution to
25 restore stability (state of balance). Therefore, the practical implication of this study is providing a basis where a decision maker
26 can picture when stability is unattainable the approach is to bring the development in the tri-nodal cities outside the risk trending
27 areas in Albay.
28

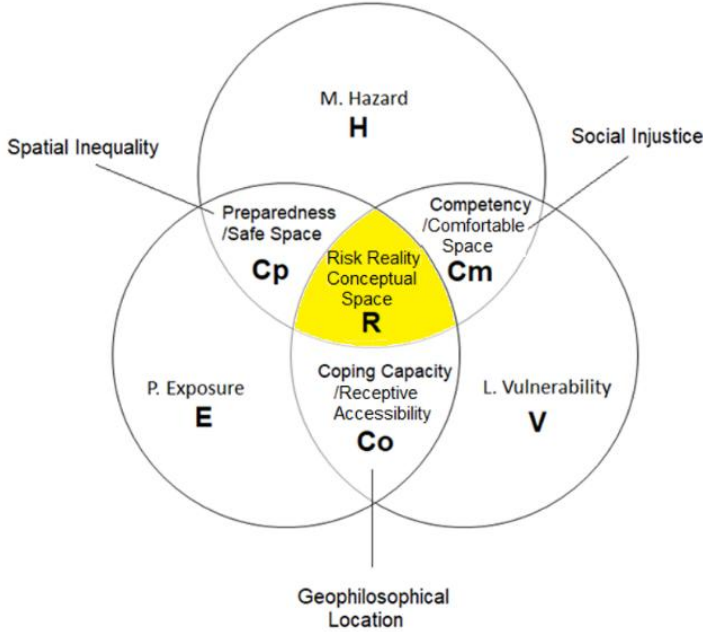
29 **Keywords:** geophilosophy, hotspots, coldspots, hexagonal bin, risk quantity, risk realness

30 **1 Introduction**

31 The Philippines is the third most disaster-prone country in the world according to the World Bank where there is low
32 uptake of research and analytic thinking to inform local decision making on disaster risk management. Disaster risk
33 reduction documentation started as early as 1814, after Mayon erupted disrupting people’s lives and displacing them
34 to look for lands suitable for planting crops far from this volcano but located near rivers and accessible to outside
35 assistance.[1][3][4]. As multiple hazard events naturally re-emerge, the land morphology relatively implies physical
36 and environmental modifications, making people vulnerable to environmental changes and discovered to be
37 dangerous. [1][3][4] Evacuation-return behavior of farmers within a complete no-build-zone model (Mayon 6-Km
38 Permanent Danger Zone of Albay), allowing barangay social and institutional facilities such as schools, barangay
39 halls, and other developments turning into the new norm that contributed to the uncontrolled sprawl within the
40 permanent and extended danger zones realization of the tri-nodal spatial developments now trending in Legazpi
41 City, Tabaco City and Ligao City. [1][3][4] Undesired developments were analyzed using Open Street Map spatial
42 data as well as the uncontrolled construction of buildings along the old railroads and rights-of-way, near rivers prone
43 to flash floods carrying lahar deposits. [1][3][4]
44

45 This study sought to measure risk, residual risk, and extraneous errors, logical to the concept of assessing risk
46 reality phenomenon. This study focuses on the significance of the implementation of Sendai Framework 2015-2030
47 to link to disasters happening within the 25 km radius referenced at the crater of Mayon Volcano to reduce human
48 and economic losses by avoiding the creation of new risks in the built environment. This paper presents the
49 conceptual framework of the study, applied from a *Geophilosophical* perspective, applying the semantics to stir up
50 reasoning to quantify the risk reality, thus understanding risk reality conceptual space variables: multiple hazards,
51 landscape vulnerability, passive exposure, preparedness, competency, and coping capacity. [1] [5][7][8]

52 Fig.1, where *H* symbolizes the combined scores of multiple hazards in Albay. The *V* symbolizes the combined
 53 scores for landscape vulnerability, which characterizes the condition of a piece of geographically enclosed land ajar
 54 to alteration (physical changes) brought by floods, bank erosion and other hydrological related hazards that may
 55 occur when river discharge exceeds its channel's volume, causing the river to overflow onto the downstream alluvial
 56 flats as well as the coastal area that convey different states of discomfort, security, worries, distress, angst, and more.
 57 Landscape vulnerability is a variable to quantify risk reality. [1][4][6][9][10] The *E* symbolizes the combined scores
 58 which measure the static position of dwelling structures, or tangible human assets that may be sited in hazard-prone
 59 areas likely to experience hazard events of different magnitudes. [1] [4][6][9][10] The preparedness, competency,
 60 and coping capacity variables carries the score that characterizes the overall capability of the local government in
 61 terms of income classification of LGUs approved by the Department of Finance to substitute the varying data
 62 associated with risk reduction and local growth.[1] [4][6][9][10] The preparedness (*Cp*) was linked with the spatial
 63 equality in terms of mitigation interventions, on the contrary one the landscape vulnerabilities are unmitigated, this
 64 variable is then linked with unsafe conceptual space. [1] [4][6][9][10] The competency (*Cm*) was linked with the
 65 social injustice in terms of competency to live comfortably which characterizes the general population repetitively
 66 evacuated or relocated to avoid any fatal accidents at times their lives are affected by hazard events such as volcanic
 67 eruption, flooding and so on. Also, competency variable was linked with careful selection of comfortable conceptual
 68 space that plainly connecting the people to the place of work and social support facilities.[1] [4][6][9][10] The
 69 comfortable conceptual space is also linked with the social injustice in terms of spatial accessibility (road and/or
 70 tape drive access) characterizing the general demands of the elderly, youngsters, significant women, PWD,
 71 displaced, exposed and other deprived people. [1] [4][6][9][10] The coping capacity (*Co*) was linked with the
 72 receptive accessibility variable. It is also spatially linked with active exposure and preparedness at all levels of risk
 73 reduction management. [1][4][6][9][10]
 74



75
 76 **Fig.1 Risk Reality Conceptual Space (Abante, 2020)**
 77

78 The Y-junction of the Gärdenfors-inspired conceptual spaces are attributed to the three (3) paired variables that
 79 are logical where risk reality is expressed as Risk → function (Multiple Hazards, Landscape Vulnerability, Passive
 80 Exposure, Preparedness, Competency, Coping Capacity) where *H* → multiple hazards; *V* → Landscape
 81 Vulnerability; *E* → passive exposure; *Cp* → preparedness (tied with safe conceptual space); *Cm* → Competency
 82 (tied with comfortable space); and *Co* → Coping capacity is tied with receptive accessibility).
 83 [1][4][6][9][10][31][32][33] [35][36][37][38][39][40][41][42][43]
 84

86 **2 Methods**

87 The study was designed to contextualize and examine the on risk hotspots and coldspots to quantify risk realities
 88 suffered by National Housing Authority (NHA) resettlement sites in Albay using GIS overlay and hexagonal
 89 binning technique to store and sort information to assess spatial patterns and quantify risk elements' statistical data
 90 to determine where the risk hotspot and coldspot are located using the ArcGIS's Getis-Ord Gi* Statistical and
 91 Moran's I Test. The researcher put together *Metatheorems* objects and parameters to requisite to perform the
 92 following: risk-enhanced resettlement site selection modeling; review the risk realness that is reliant to the
 93 computational risk reduction; and test the proposed site selection model parameters for settlement or resettlement
 94 sites as well as to examined the actuality of *Geophilosophical* realism of assessing the potential risk recurring in
 95 addition to the accumulated residual risk from past hazard events.

96 **2.1 Organizing Primary Spatial Data.**

97 Primary data were collected from OpenStreetMap and published spatial data by government line agencies. The input
 98 data were classified into ordinal scale having an ordering rating and organized to depict in a vector data formal
 99 language supported by the database built-in the GIS software used in characterizing risk elements' features it
 100 represents. In processing and quantifying the risk reality as well as selecting safe space, comfortable space, and
 101 accessible space or suitable sites for settlement/resettlements, binning techniques proved storing weighted values
 102 were achieved using the binning parameters as shown in Fig. 2.
 103

Risk Reality		Class	Very High Risk	High Risk	Moderate	Low Risk	Very Low Risk
		Description	95 to 99% Hotspot	90 to 95% Hotspot	Neutral	90 to 95% Coldspot	95 to 99% Coldspot
Risk Element	Multiple Hazards	Quantity	≥ 500	≥ 450 < 500	≥ 180 < 450	≥ 60 < 180	< 60
		Description	Very High Multiple Hazards	High	Moderate	Low	Very Low
	Landscape Vulnerability	Quantity	≥ 13	≥ 10 < 13	≥ 8 < 10	≥ 5 < 8	< 5
		Description	Critical Condition	Somewhat Unsafe Condition	Neutral	Somewhat Safe	Stable Space
	Passive Exposure	Quantity	5	4	3	2	1
		Description	Critical location	Unsafe location	Neutral	Somewhat Safe Location	Safe Location
	Preparedness	Quantity	5	4	3	2	1
		Description	Unprepared	Insufficient Preparedness	Neutral	Somewhat Prepared	Prepared
Competency	Quantity	5	4	3	2	1	
	Description	Incompetent	Somewhat Incompetent	Neutral	Somewhat Competent	Competent	
Coping Capacity	Quantity	5	4	3	2	1	
	Description	In bad condition	Poor Coping Capacity	Neutral	Somewhat High Coping Capacity	High Coping Capacity	

104 **Fig. 2 Risk Reality Binning Parameters (Abante, 2020)**

105
 106
 107 The multiple hazards aggregated scores are classified into five classes regarded as very high to extremely high,
 108 high, moderate, low and very low to absent. The landscape vulnerability aggregated scores are separated into five
 109 classes regarded as very high to extremely high, high, moderate, low and very low to absent. The passive exposure
 110 were classified into 5 classes, although in this case study the interpretation of critical locations are areas near or
 111 within 100 m reckoned from the OSM building footprints and/or OSM road centerlines to also picture where the
 112 development or sprawl are located. The preparedness, competency and coping capacity were classified into five
 113 classes regarded as very high to extremely high, high, moderate, low and very low to absent.
 114

115 The risk reality was regarded as the location or bin where Hotpot is possible and likely. It was interpreted as the
 116 multiple hazards variables having to with any of the following: unstable slopes; critical elevations; regular flooded

117 areas were given 100 weights, soil erosion prone areas which were based on soil characteristics, areas near riparian
118 rivers were given 20 weights, foreshore extent altered by storm surge were given 20 weights, areas susceptible to
119 geomorphological changes cause by Lahar, areas susceptible to Lava were given 100 weights. OSM Buildings and
120 roads coincidence (passive exposure) which were given the highest score and were extracted by buffering the lines
121 (OSM road) and polygons (OSM buildings) with 100 meters to represent nearness or density using Geoprocessing
122 Mapping tools of ArcGIS. Preparedness, Competency and Coping Capacity were assumed comparable to the income
123 classification of cities and municipalities in Albay to model risk hotspots, but this variable may partiality affect the
124 risk hotspot analysis, on the other hand these variations also were assumed at the same level or equitable to 1 up to
125 5.

126 2.2 Risk Reality Contextualization

127 In this study, risk reality refers to the quantified risk state where the function (risk reality) ~ multiple hazards,
128 landscape vulnerability, passive exposure, preparedness, competency, and coping capacity. Risk Realness refers to
129 the state of being at risk. The contextualization was necessary to portray the risk reality parameters that is geocentric
130 and grounded golden ratio and golden triangle that disclosed the vertices of resiliency that were reckoned at the
131 geometric center. The risk realness was regarded as a space promoting safety and protection. It also refers to the
132 state of being at risk wherein the state of actuality or existing situation is objectively lucid in the physical
133 environment where limits are contained in a hexagonal-shaped area whose segments are measured equidistant at 500
134 m.

135 2.2.1 Risk Reality Geometric center

136 In this study, the conceptualization of the geometric center was grounded by the Fibonacci Golden Ratio and Schoen
137 Golden Triangle. The geometric center is where the risk reality is at 0.008 units. It is regarded to be a resilient space
138 or a Gärdenfors-inspired conceptual space when it conforms to the three criteria: safe, comfortable, and accessible
139 space. Table 1 and Fig. 4 shows that the geometric center is positioned at plane coordinates x_0, y_0 . It pertains to the
140 vertex of the first isosceles triangle Δ_1 → lowest risk reality quantity highest risk reality quantity $H \times V \times EC_p \times c$
141 $C_m \times C_o \times 1 \times 1 \times 15 \times 5 \times 5 \times 1$ 125 0.008 near zero risk reality quantity proving that the vertex of resiliency is
142 significant when risk reality quantity is nearing zero.

143 2.2.2 Risk Reality Phi

144 The base line segment AB, where the object theorem is written as line segment AC → line segment AB →
145 125 segment quantity units → also regarded as the Risk Location Quotient (RLQ) unit. When $R > 125$ risk quantity
146 regarded as exceeds the upper limit in quantifying risk reality it is regarded that the computation result defies the
147 golden ratio. It is interpreted as an end which leads to a new beginning moving from one sensitive phase to a more
148 intense risk level because the risk reality → $125 \neq$ Fuzzy Risk Reality > 125 .

149 This study proved that the receptive-responsive-stability isosceles $\Delta \equiv$ unreceptive-unresponsive-socio-spatial
150 risk reality isosceles $\Delta \rightarrow$ congruent (\equiv) Socio-spatial Fuzzy Reality isosceles Δ are congruent (\equiv) when
151 grounded by the Fibonacci Golden ratio and Schoen Golden triangle, where C → Vertex of Resiliency → Angle
152 kappa → 36° , and AC → BC are asymptotic quantity segments with angle Alpha → α → angle Beta → $\beta \rightarrow 72^\circ$
153 and the φ upper limit → 125 and φ lower limit → 1 is regarded for risk reality → hotspot, thus when $\varphi > 125$ it is
154 regarded to represent the hotspot → Risk Fuzzy Reality and when $\varphi < 1$ it is regarded to represent information on
155 resiliency or risk coldspot.

156 By diagramming all the segments' complex numbers, vertices draw from asymptotic segments by similar
157 triangle technique where angles: $36^\circ, 72^\circ, 108^\circ, 144^\circ, 180^\circ, 216^\circ, 252^\circ, 288^\circ, 304^\circ$ and 324° were revealed by
158 drawing the parallel (//) lines or perpendicular lines which started the diagramming in the geometric center where R
159 → 0.008 positioned at coordinates x_0, y_0 . The *Metatheoretic* presentation of stability and/or asymptotic line
160 segments of the series of Isosceles Δ_s is regarded continuous connectivity of φ when segments of the $\Delta_s \rightarrow$ base
161 of the Δ representing the stability segment quantity → asymptotic segments representing the receptiveness and/or

168 responsiveness → 1:1 ratio → when $125 < \varphi \geq 1$ → it represent risk reality, thus when $\varphi > 125$ is regarded as
 169 risk fuzzy reality.

171 Analyzing the stability → φ → 1:1 ratio → regarded as receptiveness-responsiveness proportion → 1 to the risk
 172 reality → $\varphi \rightarrow \frac{125 < \varphi \geq 1}{125 < \varphi \geq 1}$ Ratio regarded as unreceptiveness-unresponsiveness proportion → risk reality → $125 < \varphi$

173 ≥ 1 , the φ result is regarded to a *Metatheorem* for Phi →

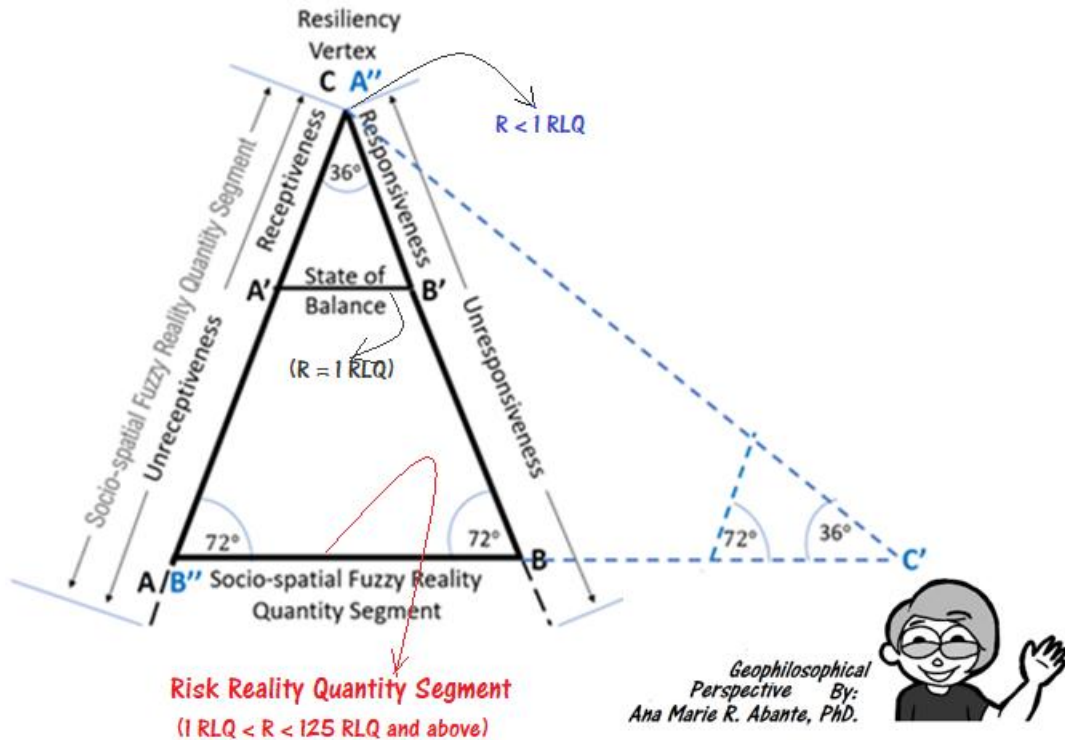
174 $\varphi \rightarrow \frac{\text{Risk Hotspot (Upper Limit)}}{\text{Risk Fuzzy Reality (125/2Cosine72°)}} \rightarrow \frac{\text{Risk Hotspot (Upper Limit)} + \text{Risk Fuzzy Reality (Risk Hotspot Upper Limit/2Cosine72°)}}{\text{Risk Hotspot (Upper Limit)}}$

175 → $\frac{\text{Risk Hotspot(Upper Limit)}}{\text{Risk Fuzzy Reality (}\frac{125}{2\text{Cosine}72^\circ}\text{)}} \rightarrow \frac{\text{Risk Hotspot (Upper Limit)} + \text{Risk Fuzzy Reality (Risk Hotspot Upper Limit/2Cosine72°)}}{\text{Risk Hotspot (Upper Limit)}}$

176 → $\frac{125}{R (125/2\text{Cosine}72^\circ)} \rightarrow \frac{125 + R(125/2\text{Cosine}72^\circ)}{125} \rightarrow \frac{2\text{Cosine } 72^\circ}{R} \rightarrow 1 + \frac{125R}{2\text{Cosine}72^\circ} \rightarrow \text{Phi } \varphi = R^2 + \frac{2\text{Cosine}72^\circ R}{AB} - \frac{(2\text{Cosine } 72^\circ)^2}{AB}$

177

178



179
 180 **Fig. 3.** Risk Reality Isosceles Δ Grounded by Schoen Δ (Abante, 2020)

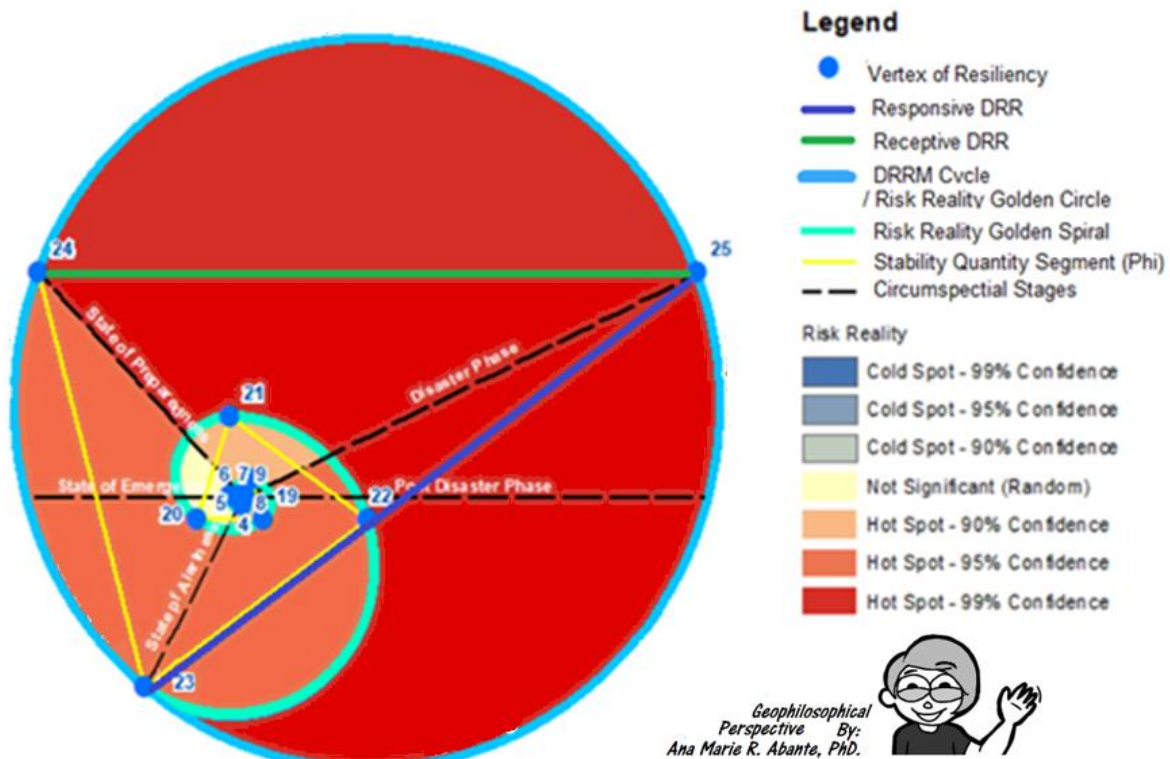
181
 182 The study proved that a spiral drawn after connecting the 25 vertices of resiliency of respective isosceles Δ s as
 183 shown in Table 1 when reckoned at the geometric center created a perfect circle when adding two more isosceles
 184 triangles. Table 1 proved that the geo center of risk reality is not at the centroid of a circle. The risk reality circle was
 185 a result of interconnecting the 27 arcs (spiral), then it continuous to loop once it formed the risk reality circle
 186 keeping the Risk Reality Phi, mathematically written as

187
 188
$$\text{Risk Reality Phi } \varphi \rightarrow R^2 + \frac{2\text{Cosine}72^\circ R}{AB} - \frac{(2\text{Cosine } 72^\circ)^2}{AB} \rightarrow R^2 + 0.00494427R - 0.00305572. \quad (1)$$

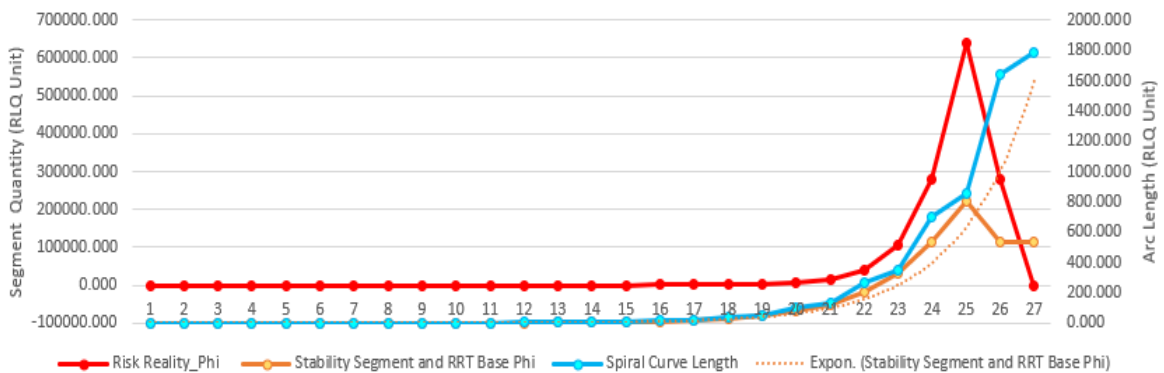
189
 190 Fig. 4 revealed the relationships of the geometric center relative to the stability as shown in Fig. 3. This study
 191 bring to light when the risk reality is one unit it depicts stability. Table 1 divulged the risk reality lower and upper

192 limits are consistent with the geometric center and spiral tail, respectively. The geometric center of the risk reality as
 193 shown in Fig. 4, and Fig. 6 are not located at the centroid of the risk reality circle that is grounded by Fibonacci
 194 Golden Ratio and Schoen Golden Triangle. The risk reality circle also revealed the asymptotic lines connecting the
 195 vertices segments 24 and 25 upward direction (following the flow from the geometric center, while the segments 25
 196 and 26 downward direction where the flow also referred to the geometric center disclosing where the stability at
 197 segment 25 plunged to a length identical to stability segment 23.

199 Fig. 4 substantiate the risk reality quantity in terms of arc lengths. These arc lengths are keys to measure the
 200 prevention, mitigation, preparedness, response, and recovery quantity units (arc lengths) to obtain risk reality at one
 201 unit hinting a stability. The line of stability in this study refers to the fulcrum of the asymptotic quantity segments
 202 (Phi) depicting the Receptive-Responsive DRRM as shown in Fig. 6.
 203



204
 205 **Fig. 4 Risk Reality Circle Grounded by Fibonacci Golden Ratio and Schoen Golden Triangle (Abante, 2020)**
 206
 207
 208



209
 210 **Fig. 5 Risk Reality Quantity Chart (Abante, 2020)**

211
212 2.2.3 Vertices of Resiliency

213 The vertex of resiliency refers to the point (geometry) where segment receptiveness and segment responsiveness are
214 measured at approaching Sine 18° where Risk reality is equal to one, at an angle 36° where the opposite segment is
215 regarded as the state of balance line of the golden (isosceles) triangle as shown in Fig 3 and Fig. 5. The vertices of
216 resiliency disclosed the relationships of the following: geometric center with risk reality equal to 0.008 unit
217 positioned at 0.0; stability line with risk reality equal to one unit; risk reality upper limit with risk reality equal to
218 125 unit positioned at the end (spiral tail) shown in Table 1 and Fig. 4. The index table also revealed the 27
219 segments that are regarded as the baselines of the 25 isosceles triangles having 72° asymptomatic angles and 36°
220 vertex angles. The spiral tail rests on the 23rd vertex. It is where the last arc connects the 25th vertex with 23rd and 24th
221 vertices. The line segment connecting the 23rd and 24th vertices hinted at the longest stability line as illustrated in Fig.
222 3, Fig. 4, and Fog. 5.

223 **Table 1.** Vertices of Resilience Index Grounded by Grounded by Golden Ratio and Triangle. (Abante, 2020)

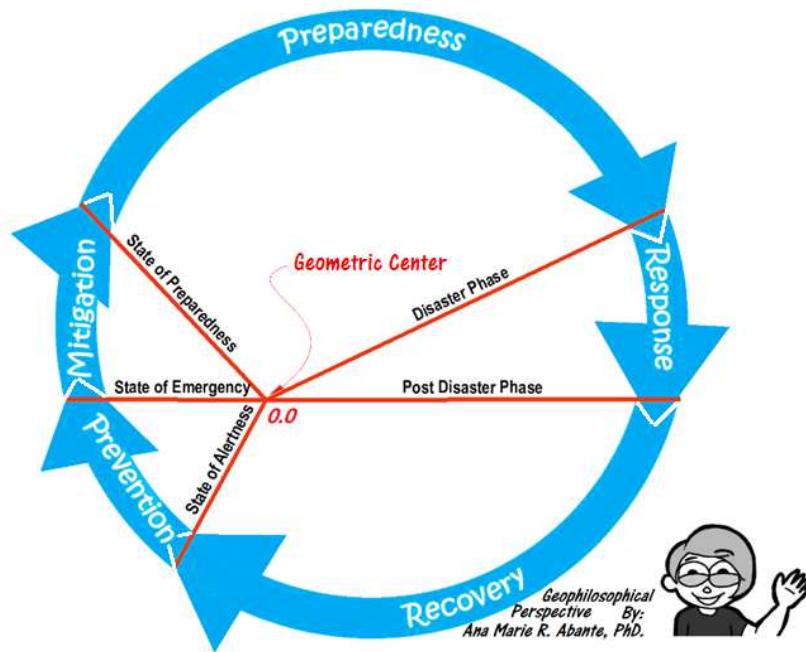
ID	Series of Resiliency Vertices			Risk Reality Golden Triangle			Risk Fuzzy Reality Phi	Spiral Curve (Arc Length)	Risk Conceptual Space (RRT Area in RLQ units)	Remarks	
	Vertex and Asymptotic Segments		Vertex X	Vertex Y	Receptiveness Segment Quantity	Responsiveness Segment Quantity					Risk Reality Segment (RRT Base) Phi
1	Vertex 1	Vertex 1 of Δ1	-0.004	0.013	0.013	0.008	0.008	-0.003	0.009	0.000	Geometric Center
2	Vertex 2	Vertex 2 (When AB =AC = BC of Δ2)	0.013	0.000	0.022	0.013	0.013	-0.003	0.018	0.000	
3	Vertex 3	Vertex 3 (When AB =AC = BC of Δ3)	-0.015	-0.021	0.035	0.022	0.022	-0.002	0.023	0.000	
4	Vertex 4	Vertex 4 (When AB =AC = BC of Δ4)	-0.032	0.033	0.057	0.035	0.035	-0.002	0.046	0.001	
5	Vertex 5	Vertex 5 (When AB =AC = BC of Δ5)	0.059	0.033	0.092	0.057	0.057	0.000	0.060	0.003	
6	Vertex 6	Vertex 6 (When AB =AC = BC of Δ6)	0.013	-0.108	0.148	0.092	0.092	0.006	0.121	0.007	
7	Vertex 7	Vertex 7 (When AB =AC = BC of Δ7)	-0.181	0.033	0.240	0.148	0.148	0.020	0.158	0.018	
8	Vertex 8	Vertex 8 (When AB =AC = BC of Δ8)	0.133	0.261	0.388	0.240	0.240	0.056	0.317	0.047	
9	Vertex 9	Vertex 9 (When AB =AC = BC of Δ9)	0.327	-0.336	0.628	0.388	0.388	0.150	0.415	0.122	
10	Vertex 10	Vertex 10 (When AB =AC = BC of Δ10)	-0.689	-0.336	1.016	0.628	0.628	0.395	0.830	0.319	
11	Vertex 11	Vertex 11 (When AB =AC = BC of Δ11)	-0.181	1.228	1.644	1.016	1.016	1.035	1.086	0.836	
12	Vertex 12	Vertex 12 (When AB =AC = BC of Δ12)	1.972	-0.336	2.661	1.644	1.644	2.709	2.173	2.188	
13	Vertex 13	Vertex 13 (When AB =AC = BC of Δ13)	-1.511	-2.866	4.305	2.661	2.661	7.090	2.844	5.728	
14	Vertex 14	Vertex 14 (When AB =AC = BC of Δ14)	-3.664	3.759	6.966	4.305	4.305	18.553	5.688	14.995	
15	Vertex 15	Vertex 15 (When AB =AC = BC of Δ15)	7.607	3.759	11.271	6.966	6.966	48.556	7.446	39.257	
16	Vertex 16	Vertex 16 (When AB =AC = BC of Δ16)	1.972	-13.586	18.237	11.271	11.271	127.093	14.893	102.778	
17	Vertex 17	Vertex 17 (When AB =AC = BC of Δ17)	-21.901	3.759	29.508	18.237	18.237	332.682	19.495	269.075	
18	Vertex 18	Vertex 18 (When AB =AC = BC of Δ18)	16.726	31.823	47.746	29.508	29.508	870.889	38.990	704.451	
19	Vertex 19	Vertex 19 (When AB =AC = BC of Δ19)	40.599	-41.650	77.254	47.746	47.746	2279.891	51.038	1,844.283	
20	Vertex 20	Vertex 20 (When AB =AC = BC of Δ20)	-84.401	-41.650	125.000	77.254	77.254	5968.605	102.077	4,828.394	
21	Vertex 21	Vertex 21 (When AB =AC = BC of Δ21)	-21.901	150.705	202.254	125.000	125.000	15625.615	133.620	12,640.889	Vertex C
22	Vertex 22	Vertex 22 (When AB =AC = BC of ΔABC)	242.853	-41.650	327.254	202.254	202.254	40907.770	267.240	33,094.273	Vertex C'
23	Vertex 23	Vertex 23 (When AB =AC = BC of ΔACC')	-185.528	-352.888	529.508	327.254	327.254	107096.924	349.821	86,641.931	Vertex C'' & Spiral 23 (Tail)
24	Vertex 24	Vertex 24 (When AB =AC = BC of ΔCC'')	-392.639	420.062	800.216	529.508	529.508	280381.810	699.643	211,860.672	Vertex C'''
25	Vertex 25	Vertex C''	878.346	420.062	1270.985	800.216	800.216	640350.241	855.399	508,531.521	Vertex C''''
26					1270.985	529.508	529.508	280381.810	1,639.514		
27					1270.985	529.508	529.508		1,782.081		Spiral 25

224
225 2.2.4 DRRM-Circumspectial Isometric Stages Grounded by Risk Reality Phi

226
227 The DRRM-Circumspectial Isometric Stages is presented to advocate the pairing of the five Circumspectial stages
228 with the five DRRM cycles to measure risk reality through the geospatial information model that verbalizes that
229 stability that is logical to site selection (space allocation). [1][4][5][6][9][10][11][12][32][33] While the DRRM
230 cycle is itemized into prevention, mitigation, preparedness, response, and recovery, the circumspectial stages
231 reckons where to twitch these five risk reduction interventions. [1][6][9][10] The five circumspectial stages are
232 regarded as the state of alertness, state of emergency, state of preparedness, disaster phase and post-disaster phase.

233 [1][6][9] The risk realness (geospatial) information give a rough idea of the complex interaction between a potential
 234 damaging physical event (regarded as multiple hazards in this study) combined with the vulnerability of NHA
 235 resettlement sites (where landscape critical condition and exposure (situation or nearness) are quantified and
 236 classified into hotspot, random or coldspot .[1][11][12]
 237

238 Fig. 6 is grounded by Fig. 5 wherein the arc lengths are measurements of the DRRM cycle: prevention,
 239 mitigation, preparedness, response, and recovery. These five arc lengths concur with the five line-segments of the
 240 DRRM Circumspectial stages that are reckoned at the geometric center: State of Alertness; State of Emergency;
 241 State of Preparedness; Disaster Phase and Post Disaster Phase are reckoned at the geometric center of the risk reality
 242 circle. The Stability line-segment is measured from the end nodes of line-segments ‘State of Alertness’ (Vertex 23 in
 243 Fig. 4, Fig.5 and Table 1 as spiral tail) and ‘State of Preparedness’ (Vertex 24 in Fig. 4, Fig.5 and Table 1) measured
 244 from the geometric center. Preparedness is bounded by an arc line (risk reality partition) measured from Vertex 24 to
 245 Vertex 25 (as shown in Fig. 4, Fig. 5 and Table 1). Similarly, the line segment connecting Vertex 24 and Vertex 25
 246 concur with the receptive risk reduction segment quantity (asymptotic segment (Phi as shown in Fig. 4) of the small
 247 Risk Reality Triangle (RRT) as shown in Fig. 3). Likewise, Vertex 25 and Vertex 23 concur with the responsive risk
 248 reduction segment quantity (asymptotic segment (Phi as shown in Fig. 4) of the small Risk Reality Triangle (RRT)
 249 as shown in Fig. 3). The Disaster Phase line segment in Fig.6 and Fig. 3 is measured from Vertex 25 to the
 250 geometric center. A horizontal line is drawn to create the partition of quick response and recovery. A line is drawn
 251 parallel to the Post Disaster Phase and measured from the geometric center is called the state of emergency. The
 252 researcher presents the State of Calamity can be drawn in between the State of Preparedness and Disaster Phase. The
 253 State of Calamity is seen as reliant on the State of Preparedness. Considering the preparedness remains a variable
 254 and perceived to be constantly changing, the five partitions relatively changes as hazard events intensifies and/or
 255 exposure continue to increase.
 256
 257



258
 259 **Fig. 6 DRRM-Circumspectial Isometric Stages Parameter (Abante, 2020)**

260 **2.3 Risk-enhance Resettlement Site Selection Modeling**

261 The risk-enhance resettlement site selection modeling using geospatial information and ArcGIS software tested
 262 the following: *Metatheorems* object grounded by geophilosophical perspective on risk reality; Risk Reality Context
 263 Model Grounded by Golden Spiral; and Site Selection Modeling Grounded by Risk Reality Context Model.

264 [1][26][27][28][29][30] The Binned Risk hotspot and coldspot was regarded to mimic the risk reality in Albay.
265 [1][7][8][26][27] The geospatial information (Geoinformation) data model built up for this study revealed the non-
266 exercise of the hexagonal binning technique leads to complexities in quantifying risk and evaluating the risk reality.
267 [1][5][6][9][10][11][12][26][27][28][29][30] The binned statistical data were processed using the Gates Ord Gi*
268 (geostatistical tool) to analyze the neighborhood of values for risk and its constituents. The Moran's index
269 characterizes weight matrices significance for autocorrelation analysis. The z-scores were categorized into 7 levels
270 of significance. The geospatial aspects and impact of data as illustrated and pinpoint the causes of specific
271 geographic patterns that were reliant to the visual inspection and image interpretations were limited to the
272 knowledge of the researcher's technical experiences as a photogrammetrist, cartographer, GIS specialist, geodetic
273 and civil engineer and an environmental planner practicing land use planning) to interpret the risk variables and sub-
274 variants.

275 2.3.1 Hexagonal Binning Technique.

276 The risk hotspots and coldspot in Albay highlights the hexagonal binned data disclosing where the hotspots in terms
277 of: multiple hazards binned geoinformation, landscape vulnerability binned geoinformation, passive exposure
278 binned geoinformation, and capability (Preparedness, Competency and Coping Capacity) binned non-spatial data
279 (attributes). [1][17][18] The data binning was reckoned 25 km from the crater of Mayon Volcano in Albay where the
280 urban development trends (and sprawl) and constraints (risk hotspots) are located using hexagonal bin maps.
281 Hexagonal bin map (tessellated cells created using ArcGIS 10.8 version) is fishnet-like or honeycomb-like
282 hexagonal polygons arranged perfectly to store and sort the risk reality information distributed in the 25 resettlement
283 sites in Albay. The 1,541 hexagonal bins which covers the 25 km radial distance measured from the crater of Mayon
284 Volcano having an area of 154,160.14 hectares, plays an important role in analyzing the spatial variation of risk
285 reality in Albay. Risk reality was measured in every 100 Ha of land to depict the degree of confidence and rendering
286 of risk hotspot and coldspot spatial patterns. Visualization of risk reality on the basis (real physical space) is doable
287 using hexagonal bins with 100 Ha area coverage, wherein an average person with a 0.50-meter pace factor can walk
288 a 500-meter radius (distance) or take 1,000 steps with 3-meter/second speed can measure the one-side of the
289 hexagon in just 3-minutes or it takes 18 minutes to walk round a flat physical space regarded as a hexagonal bin.
290 Fig. 7 demonstrates that the hexagonal bins (circularity of a hexagon grid) is a better way to represent data more
291 naturally than square grids. The hexagon (bin) polygon (rather than a perfect circle) is a tessellated polygon regarded
292 as a Hexagonal bin in this study.
293



294 **Fig. 7** Tessellated Hexagonal Bins (Polygons)
295

296 2.3.1 Situational Analyses.

297 The higher portion of the Mayon Volcano is a natural park (located within the permanent danger zone) reserved for
298 the conservation of native plants and animals, their associated habitats and cultural diversity. At least a 24.4 km road
299 network that leads access to the 8 km extended danger zone (remain an alienable and disposable and desirable for
300 production forest uses. Without seeing the force of sprawl as people go forward to develop their lands and
301 constructions of buildings near the gullies, alluvial fans at the foot slopes of the volcano, old railroads which were

302 ruined by repetitive volcanic eruptions, people remain playing against disaster risk as multiple hazard events
303 iteratively happen again and again.

304
305 The undesired buildings were built along rights-of-ways such as barangay/purok roads, farm-to-market roads,
306 trails and tracks of trucks hauling the gravels and sands needed to develop cities and municipalities, dikes,
307 evacuation routes, and so on. [1][3][4][31] The barangay (village) nodal centers or the location of the barangay halls
308 is interconnected with road and road-like patterns. Density of buildings surrounding the barangay nodal centers
309 varies depending on the slope, lift and other landscape features such as river and its bank erosion due to severe
310 rainfalls. [1][4]

311

312 2.3.2 Risk Areal Differentiation

313 In this study this refers to the method to get the difference between two calculated risk quantities, wherein the
314 negative residual value implies worsen risk reduction actions are applied to reduce risk; In contrast, the practical
315 implication of positive residual affirms corrective risk reduction measures. [34] The geographic location (point
316 features) of the 25 resettlement sites was overlaid with the hexagonal bins (polygon features) using ArcGIS's
317 Geoprocessing Tool. The intersection of point and polygon features made possible transferring the hotspot, random
318 and coldspot z-scores attributes from polygon to point map features. Then the areal differential technique was
319 applied to get the residual risk (ΔR).

320 2.4 Receptive and Responsive DRRM Review

321 The Receptive-Responsive DRR Isometric Index as shown in Fig. 8 was created to simplify risk reduction
322 parameters. It was tested and applied to review the relationship of the safe conceptual space reliance with the risk
323 reality z-scores of the resettlement sites that may be safe, but not necessarily comfortable and accessible or may be
324 comfortable temporarily (somewhat located far flung) but safe or resilient area. *Metatheorems* were used to further
325 review the risk reality z-scores.[1] Notice the line formed by the cell with numerical value equal to one. It act as a
326 partition when risk reality is less than or greater than one unit.

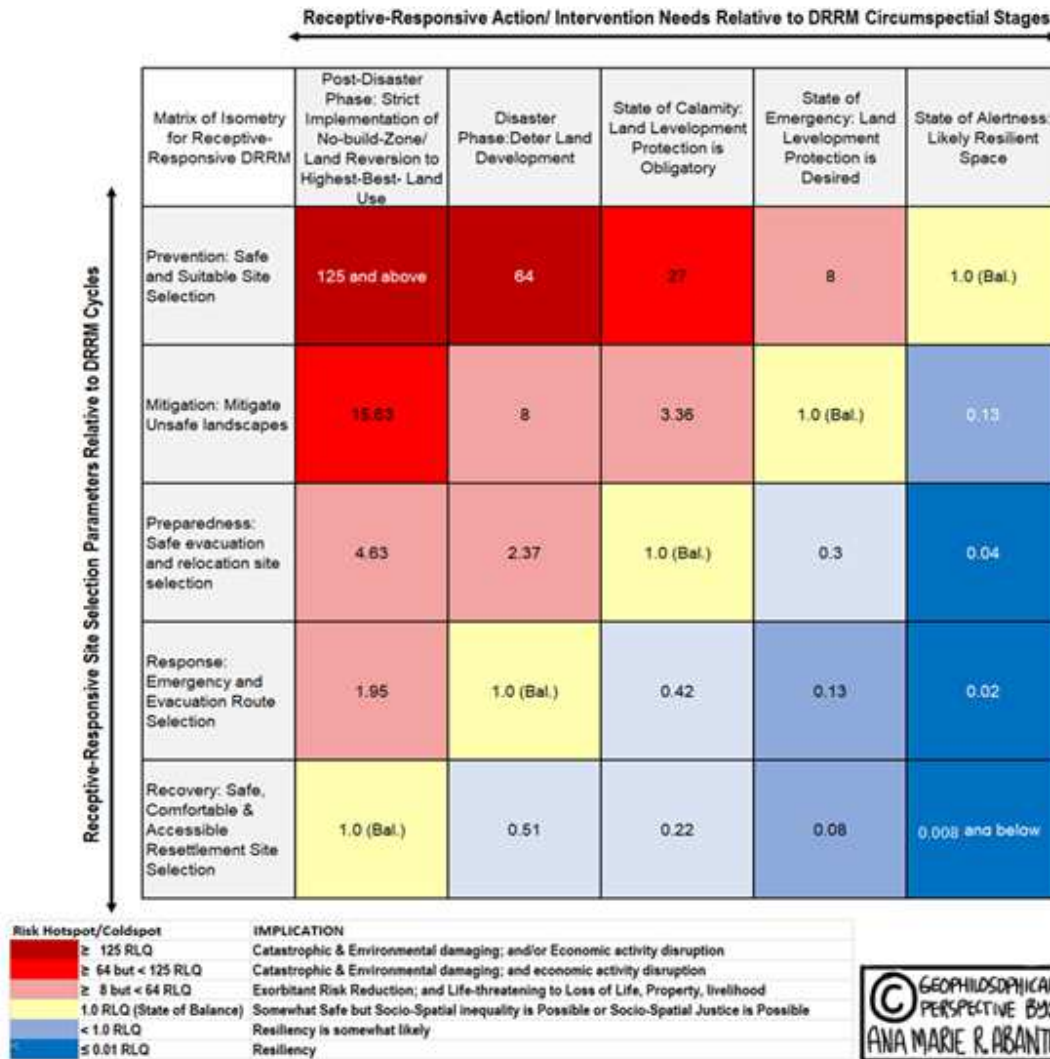


Fig. 8 Receptive-Responsive DRR Isometric Index (Abante, 2020)

327
328

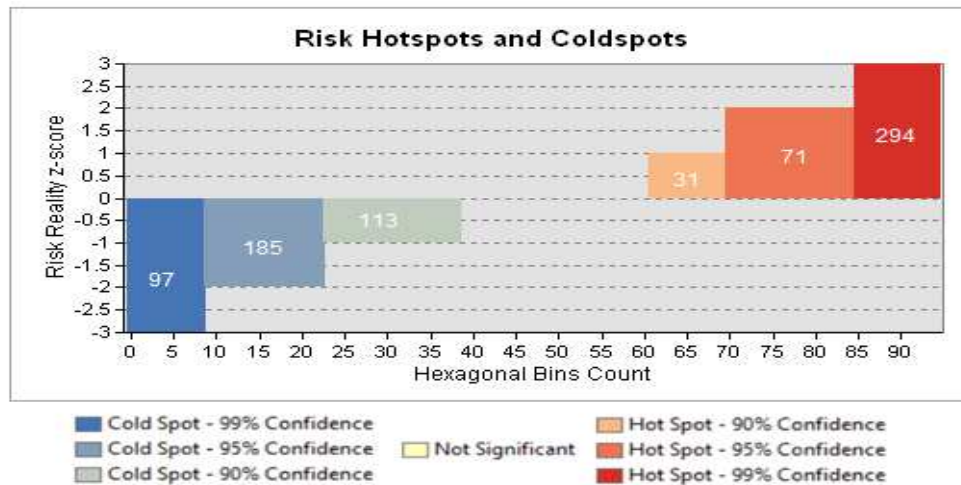
329 3 Results

330 The risk reality and trend in terms of spatial information on multiple hazards, landscape vulnerability, passive,
 331 exposure and the nonspatial information on capability are regarded as the combination of the preparedness,
 332 competency, and coping capacity of the government. The hotspot incidence in terms of 623 bins or 62,300 Ha
 333 regarded as the combined building and road incidences. Of all the risk elements this information is the independent
 334 variable of risk reality. Risk cannot exist in bins when passive exposure is nil. See the bin map at the end of the
 335 discussion. Unlike the first three (3) risk elements, the Capability is expressed as non-spatial information
 336 representing the attributions regarded as the other three (3) elements of risk, these are: preparedness, competency,
 337 and coping capacity. These elements characterize the denominator, taking the part (pairing) in cutting the multiple
 338 hazards, landscape vulnerability and exposure, the pairing are as follows: multiple hazards and preparedness,
 339 landscape and competency, and exposure and managing capacity. These pairing constitute the three (3) conceptual
 340 spaces supported by *Metatheorems*, these are: a safe conceptual space indicating there is spatial equality,
 341 comfortable conceptual space to stand for social justice, and philosophical location (conceptual space). Since the
 342 passive exposure is involved as an independent variable when paired with coping capacity hinted at the

343 geophilosophical location as a conceptual space is the most important information that connotes land utilization and
 344 zoning.

345
 346 The risk realities findings in the 25 resettlement sample sites in terms of: risk reality z-score processing result,
 347 risk reality overlay analysis result, risk realities tabulation, and visualization of risk realities in NHA resettlement
 348 sites. [1][19][20][21][22][23][24][25] The risk realities suffered by the NHA resettlement sites in Albay in terms of
 349 charting: risk reality, descriptive style, and conceptual space tabulation, risk reality suffered by NHA resettlement
 350 sites. [1][5]

351
 352



353
 354 **Fig.9 Risk Hotspots and Coldspots Bin Count**
 355

356 The more people utilize danger zones the more financial content is required to stay balanced following a zero-
 357 casualty strategy of Albay. Therefore, the bin maps for preparedness, competency and coping capacity were inputted
 358 with the income class of the urban centers and municipalities. It means each hexagonal bin is attributed to income
 359 class weighted from 1 (lowest) to 5 higher, indicating the 5% budget allocation for DRRM programs and activities.
 360 See the bin maps at the end of the discussion on risk hotspots and coldspots in Albay. This graph below disclosed
 361 the sum of risk hotspots, random/insignificant or coldspots information that connects the risk reality z-scores: 294
 362 hexagonal bins or 29,400 hectares of land are labelled as 99%, significantly hotspot, 71 hexagonal bins are labelled
 363 95%, significantly hotspot, 31 hexagonal bins are 90%, significantly hotspot, 113 hexagonal bins are 90%
 364 significantly coldspot, 185 hexagonal bins are 95% significantly coldspot and 97 hexagonal bins are 99%
 365 significantly coldspot. The ArcGIS's Getis-Ord G_i^* Statistical and Moran's I Test results also disclosed the general
 366 hotspot wherein the areas with z-scores varying from 1.65 to 1.96 cover the resettlement sites disclosed the
 367 following: Legazpi City, Ligao City, Tabaco City, Bacacay, Camalig, Daraga, Guinobatan, Libon, Malilipot,
 368 Malinao, Oas, Polangui, Sto. Domingo and Tiwi. On the contrary, the coldspots are generally depicted by z-score
 369 between <1 and $z\text{-score} \leq 2.58$ which cover the following watershed divides: Balobo (Ligao-Guinobatan area),
 370 Banwang Gurang (Camalig-Jovellar area), Ogod (Camalig-Jovellar area), Polangui (Polangui-Oas area), Quinali
 371 'A' (Camalig, Guinobatan, Ligao, Oas and Polangui area), Quinali 'B' (Malinao-Tabaco), Taque and Tiwi-Sangay
 372 area. Other fields are barely random values.

373
 374 The risk realities suffered by resettlement sites are regarded as the lack of spatial quality regarded as
 375 receptiveness is unlikely (U) and short of social injustice regarded as responsiveness is unlikely (U) where stability
 376 is reliant on the segment quantity of unreceptiveness and unresponsiveness. The N indicates no certain suffering
 377 based on the scientific data findings, although some recipients of housing projects may disagree with this geospatial
 378 information modeling results. The following research output reveals the risk realities suffered by resettlement sites
 379 in terms of the following: risk reality, descriptive trend, conceptual space tabulation, and risk reality suffered by
 380 NHA resettlement sites. Table 2 exhibit the risk realities suffered by the resettlement site in Albay: Likely (Li),
 381 Somewhat Likely (SLi) and Unlikely (U); Social Justice: Likely (Li), Somewhat Likely (SLi) and Unlikely (U);

382 Receptiveness: Likely (Li), Somewhat Likely (SLi) and Unlikely (U); Responsiveness: Likely (Li), Somewhat
 383 Likely (SLi) and Unlikely (U); and Stability: Likely (Li), Somewhat Likely (SLi) and Unlikely (U). [1] It also
 384 demonstrates where stability is unlikely regarded as suffering risks by resettlement sites. Based on scientific
 385 findings, the following suffered risk: Cullat (Daraga), Lamba (Legazpi), Ligao City, Miisi (Daraga), Oson (Tabaco
 386 City), Pinabobong (Tabaco City), Quitago (Guinobatan), Salvacion (Tabaco City), San Vicente (Tabaco), Sto.
 387 Domingo, Tabaco Housing Project, Tagaytay (Camlig), Taysan (Legazpi City).

388
 389

Table 2. Risk Realities Suffered by NHA Resettlements in Albay (Abante, 2020)

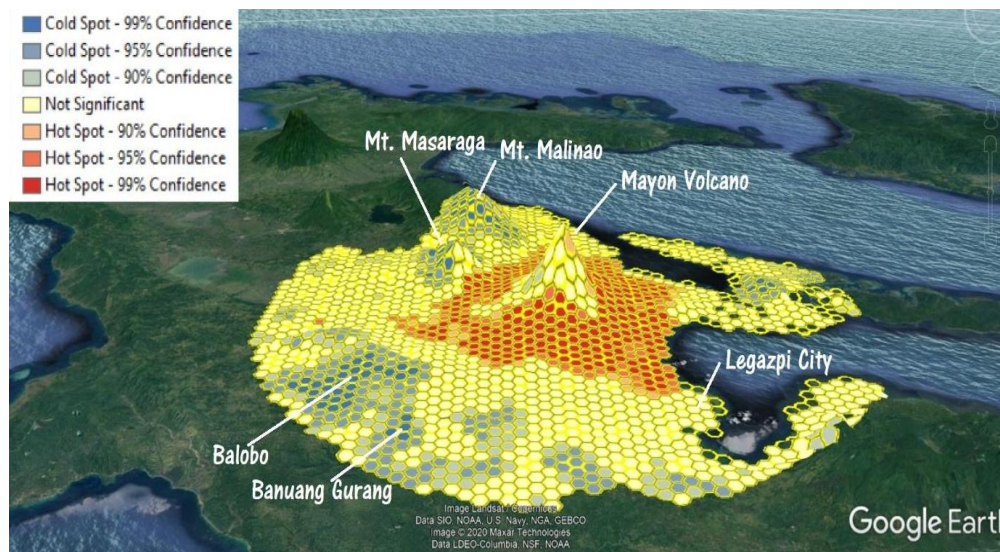
ID	NHA Resettlement Site	Present Risk Reality			Risk Trend			Receptiveness	Responsiveness	Risk Suffered
		Z-score	Risk Reality	Residual	Phi	Phi Impact	Trend			
1	Amore Resettlement Project	-1.38	C	N	N.A.	N	C	Li	Li	N
2	Banquerohan Resettlement Project Ph I	-0.66	C	N	N.A.	N	C	Li	Li	N
3	Banquerohan Resettlement Project Ph II	-1.31	C	N	N.A.	N	C	Li	Li	N
4	Bascaran Resettlement Project	-0.43	C	N	N.A.	N	C	Li	Li	N
5	Camalig Resettlement Project	-0.49	C	N	N.A.	N	C	Li	Li	N
6	Cullat Resettlement Project	3.32	H	Y	11.02	Y	F	U	U	Y
7	Daraga Resettlement Project Ph I	-0.81	C	N	N.A.	N	C	Li	Li	N
8	Daraga Resettlement Project Ph I	-0.82	C	N	N.A.	N	C	Li	Li	N
9	Daraga Resettlement Project Ph II	-0.40	C	N	N.A.	N	C	Li	Li	N
10	Lamba Resettlement Project	0.61	H	Y	0.37	Y	H	U	SLi	Y
11	Ligao Resettlement Project	2.26	H	Y	5.12	N	F	U	SLi	Y
12	Mauraro Resettlement Project Ph II	-0.55	C	N	N.A.	N	C	Li	Li	N
13	Miisi Resettlement Project	4.19	H	Y	17.53	N	F	U	U	Y
14	Oas Resettlement Project	-0.32	C	N	N.A.	N	C	Li	Li	N
15	Oson Resettlement Project	4.54	H	Y	20.61	Y	F	U	U	Y
16	Pinabobong Resettlement Project	3.40	H	Y	11.57	N	F	U	U	Y
17	Polangui Resettlement Project	-1.62	C	N	N.A.	N	C	Li	Li	N
18	Quitago Resettlement Project	1.08	H	Y	1.18	N	C	U	SLi	Y
19	Salvacion Resettlement Project	2.54	H	Y	6.44	Y	F	U	SLi	Y
20	San Vicente Resettlement Project	0.69	H	Y	0.48	Y	H	U	SLi	Y
21	Sto. Domingo Resettlement Project Ph I	0.86	H	Y	0.74	Y	H	U	SLi	Y
22	Tabaco Housing Project	0.69	H	Y	0.48	Y	H	U	SLi	Y
23	Tagaytay Resettlement Project	1.97	H	Y	3.89	Y	H	U	SLi	Y
24	Taysan Resettlement Project	-0.07	Ra	Y	N.A.	N	Ra	U	Li	Y
25	Taysan Resettlement Project	1.84	H	Y	3.40	Y	H	U	SLi	Y

390 Note: C→Coldspot; H→Hotspot; Ra →Random; F→Fuzzy Reality; Y→Yes; N→No; VH →Very High; H→High; M→Moderate; L→Low;
 391 VL→Very Low; N.A.→Not Applicable; Li→ Likely; SLi → Somewhat Likely; U →Unlikely

392 4 Discussion

393 The Risk Reality in Albay in terms of the spatial aspects of the three risk elements such as multiple hazards,
 394 landscape vulnerability and passive exposure, locate the risk hotspots or coldspots in the study area. The multiple
 395 hazards hotspots with 99% level of confidence are located within the Mayon 6 km permanent danger zone; between
 396 the 6 to 8 Km extended Mayon danger zone covering Tabaco City and Malilipot. It also includes areas near the
 397 Albay Lineament fault line crossing the town of Libon, Oas, Ligao City, Guinobatan, Camalig, Daraga, ending in
 398 Legazpi City. In terms of the landscape vulnerability, hotspots with 99% level of confidence greatly cover the 4 Km
 399 buffer area reckoned from the 6 km permanent danger zone. Measuring Passive Exposure relies on the location of
 400 building and road network where the said multiple hazards and passive vulnerable hotspot areas exist. The technique

401 on binning information on hexagonal cells reveals that about 29,400 hectares in Albay are significant risk hotspots,
 402 with 99% confidence. Also, at least 7,100 hectares of land are significant risk hotspots, with 95% confidence, and
 403 3,100 hectares are significant risk hotspots with 90% confidence. The risk hotspot areas reach up to 15 kilometers
 404 from the Mayon Volcano's crater, covering Legazpi City, Daraga, Camalig, Guinobatan, the eastern section of
 405 Ligao City, Tabaco City, Malilipot, the western portion of Bacacay and Sto. Domingo. In terms of Coldspots or
 406 areas measured to be resilient: within the 25 km radius study area measured from the Mayon's crater, the
 407 mountainous portion of Mount Malinao (covering Malinao and Tiwi), Mount Masaraga (covering western portion of
 408 Tabaco City, eastern portion of Polangui and Ligao City), mountain hill ranges of the watershed and production
 409 forest (covering Libon, Oas, southern portion of Ligao City, Guinobatan and Camalig) and Jovellar) are measured as
 410 coldspots, with 90% level of confidence.
 411



412 **Fig. 10** Risk Hotspot and Coldspot Tessellated Bins Visualization in Google Earth Platform
 413
 414

415 Although these hotspots and coldspots outline the risks in spatial aspects relative to quantifying spatial equality,
 416 the term social justice remains reliant to the nonspatial aspects of capability. [1][35][36][47][38][39][40] These non-
 417 spatial aspects include *preparedness, competency and coping capacity* of the LGUs, where preparedness,
 418 competency and competency ratings were based on income class, and the 5% mandatory fund for prevention,
 419 mitigation, preparedness, response and recovery. [1]The variations which influence risk reality to either boost local
 420 development (if risk is reduced to bearable quantity), or to a worsened state if risk realities continue accruing. [1] A
 421 worsened risk reality implies that the socio-spatial reality in terms of spatial equality, social justice accessibility and
 422 stability are unmet. [1]
 423

424 Socio-spatial reality, in terms of spatial equality, social justice accessibility and stability in the NHA resettlement
 425 sites in Albay were examined. This revealed the existence of a spreading risk in the following resettlement sites:
 426 Miisi and Cullat in Daraga ; Pinabobong, Tabaco Housing, Salvacion and Oson in Tabaco City, Taysan Phase I and
 427 II, and Lamba in Legazpi City; Ligao City; Quitago in Guinobatan; Sto. Domingo and Tagaytay in Camalig. A total
 428 of thirteen (13) out of twenty-five (25) resettlement sites in Albay are located within risk hotspot areas. Spatial
 429 equality (safe conceptual space) is unlikely (unsafe space) in all the above-mentioned resettlement sites except
 430 Taysan I in Legazpi City. In terms of Social Justice (comfortable conceptual space) are unlikely (unsafe space) in
 431 Cullat, Miisi, Oson, and Pinabobong, and the rest of the sample sites are found to be slightly likely comfortable
 432 sites. In terms of the accessibility of resettlement sites, Oson, Pinabobong and Quitago are unlikely accessible (not
 433 easily accessible), but Lamba, Miisi, Tagaytay, Taysan Phase I and II and Sto. Domingo seems slightly likely to be
 434 accessible. The nearness of Cullat, Ligao, Salvacion, San Vicente and Tabaco Housing to the social facilities mostly
 435 located in the tri-nodal cities of Albay (Legazpi, Ligao, Tabaco) place these resettlement sites likely accessible. But
 436 because these 13 resettlement sites are consequently located in risk hotspot areas, by applying the *Metatheorems* of
 437 this study, stability for these sites is unlikely.

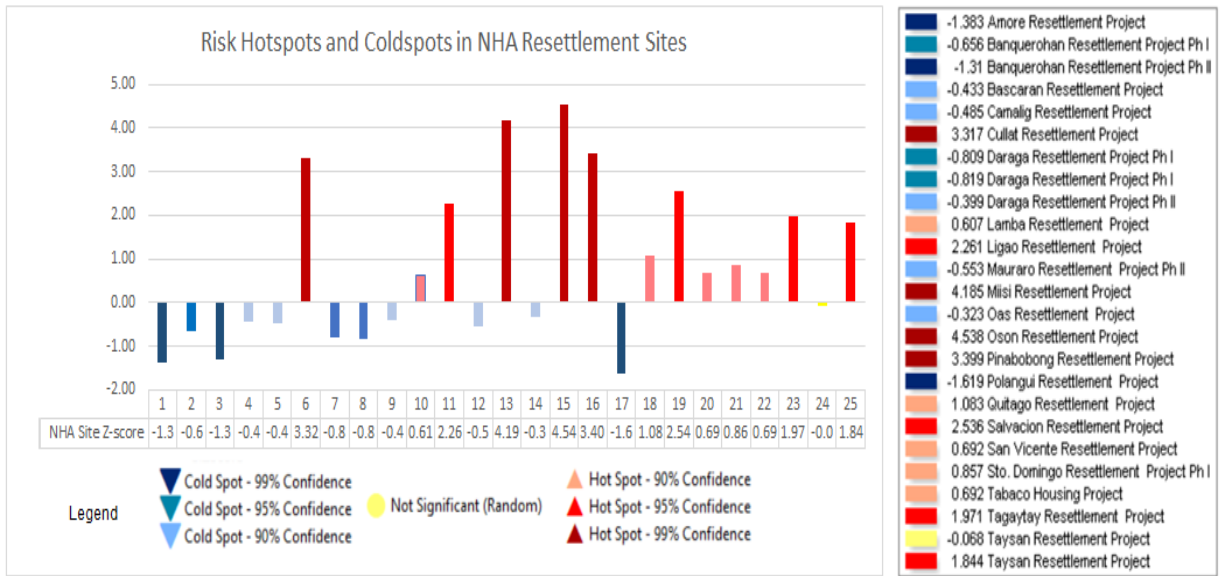


Fig. 11 Risk Realness in Resettlement Sites in Albay, Philippines

439
440
441
442
443
444
445
446
447
448

Fig. 11 presented the risk realities in terms of hotspot and coldspot to exemplify the results after overlay analysis. The risk reality are regarded as the z-scores and classification of hotspot and coldspot: Very Low indicating 95% to 99% significantly coldspot or Very Low Risk Class (VL); Low indicating 90% significantly coldspot or Low Risk Class (L); Moderate indicating random negative or positive z-score values between -89% to 89% confidence (M), High indicating 90% to 95% significantly hotspot or High Risk Class (H), and Rising Uncertainties indicating 99% significantly hotspot (VH) determine whether spatial equality is likely or not.

449
450
451
452
453
454
455
456

In tallying the risk reality values in the resettlement sites in Albay as shown in Table 2, it was revealed that fourteen (13 significantly risk hotspot and 1 insignificant value) out of the twenty-five NHA resettlement sites suffered in terms of the risk reality z-scores quantity where risk reality regarded hotspot or coldspot; Phi hinted spreading risk in resettlement sites. Moreover, out of the fourteen resettlement sites, four significantly need attention to reduce their disaster risk, these sites are: Oson and Pinabobong, in Tabaco City; and Cullat and Miisi, in Daraga town. Of these four sites, Cullat is a unique case: the hexagonal bin where this spot coincides generally characterizes the neighborhood oh high values interpreted by the Getis-Ord G_i^* statistical tool in ArcGIS 10.8 version.

457
458
459
460
461
462
463
464
465
466
467

Taking part in validating the precise location relative to the physical landscape where Cullat resettlement sits as shown in Fig. 12, it was learned the binned information on slope carries a generalized weight of 4 indicating a high landscape vulnerability value. This shows that more detailed information and smaller size of hexagonal bins can bring more variations that can improve outcomes. Consequently, Cullat resettlement site carries a higher z-score. Each hexagonal bin carries a specific numerical value regarded as Risk Reality function (multiple hazards, landscape vulnerability, passive exposure, preparedness, competency, and coping capacity). Furthermore, the result of this study acknowledges the limitations of data model carries the accuracies of 1:50000 scale input maps only to show that it fits for macro planning or risk rapid assessment. Merely the same approach in site selection may be adopted for micro planning or comprehensive risk assessment.

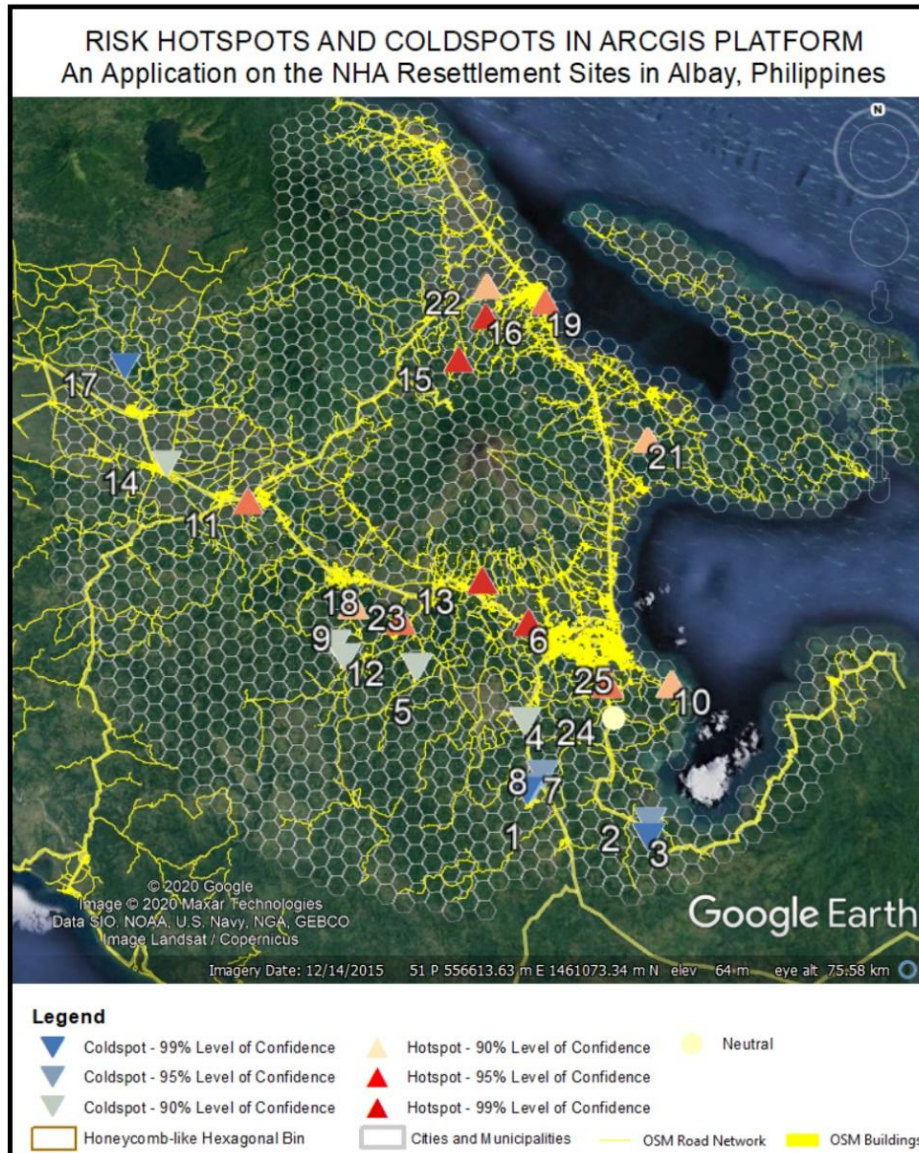


Fig. 12 Risk Reality in NHA Resettlement Sites in Albay, Philippines

468
 469
 470

471 **5 Conclusions**

472 Risk realities in terms of hotspots or coldspots is reliant on the receptive and responsive DRRM which entails an
 473 interdisciplinary thinking applying geospatial data science to characterize the multiple hazards, landscape
 474 vulnerable, and passive exposure hotspots or coldspots impacting Albay Province.
 475

476 The researcher concluded that at least 14 resettlement sites in Albay will continue to suffer if the National
 477 Housing Authority, and other relevant agencies will delay relocating exposed residents to a safe space (with respect
 478 still to the spatial equality), comfortable space (considering social justice), accessible sites approximately near the
 479 basic social services of the government. It further concluded that unreceptive and unresponsive mitigation actions
 480 affect whether the exposed population will become fully prepared or remain unprepared to withstand repetitive
 481 hazard events and the intrinsic effects of repetitive temporary evacuation of housing project beneficiaries.
 482

483 When stability is unlikely (at household, community level), meaning existing in an unsafe situation, there is a
484 larger financial requirement to capacitate the local government units. Further, that while the risk realities in the 14
485 resettlement sites will continue to accrue based on the scientific findings (grounded by *Metatheorems* Objects on
486 Stability, Risk Reality, and Risk Trends), more suffering will be experienced when risk becomes unbearable, where
487 full recovery at any level is unlikely.
488

489 As the Risk-enhanced Resettlement Site Selection Model exhibited the realness of risk, spatial equality, social
490 injustice, safe space, comfortable space, it allows visualization in the form of maps, graphs and tables revealing
491 where receptive and responsive risk reduction is greatly needed. As a final point, risk reality is quantifiable and
492 actionable, when supported by *Geophilosophical* reasoning supported by *Metatheorem* objects on risk reality where
493 stability is the fulcrum to quantify receptive-responsive risk reduction interventions

494 **Availability of data and materials**

495 N. A.

496 **Competing interests**

497 N. A.

498 **Funding**

499 The author is a faculty member and recipient of the Bicol University Human Resource Development Program..

500 **Authors' contributions**

501 Abante, A. M. R. designed the Risk Reality Conceptual Space Model for her dissertation for the Doctor of
502 Philosophy in Development Management to measure and prove the uniqueness of risk, residual risk and
503 extraneous errors that are logical to the concept of assessing risk reality (conceptual space grounded by
504 geographic concepts) phenomenon.
505

506 Abante, A. M. R. conceptualized the Risk Reality Isosceles Δ Grounded by Schoen Golden Triangle for her
507 dissertation for the Doctor of Philosophy in Development Management to prove risk reality is measurable.
508

509 Abante, A. M. R. conceptualized the Risk Reality Circle Grounded by Fibonacci Golden Ratio and Schoen Golden
510 Triangle for her dissertation for the Doctor of Philosophy in Development Management to prove that stability
511 changes as it pivots the geocentric center which hinted where the resiliency is hinged as well as proving the
512 relationships of the vertices of resiliency that are interconnected and arranged opposite of the with the stability
513 baselines of all isosceles triangles where the asymptotic segments hinted at receptive and responsive risk
514 reduction.
515

516 Abante, A. M. R. created the Vertices of Resiliency Index Grounded by Grounded by Golden Ratio and Triangle
517

518 Abante, A. M. R. designed the computational DRRM-Circumspectial Isometric Stages Framework Model needed to
519 analyze the resulting risk reality z-scores to assess risk realness stored and sorted in hexagonal bins. This
520 research output is part of her dissertation manuscript for the Doctor of Philosophy in Development Management.
521

522 Abante, A. M. R. crafted the risk-enhanced resettlement site selection modeling, a technique to review the risk
523 realness that is reliant to the computational DRRM-Circumspectial Isometric Stages Framework Model. The
524 National Housing Authority resettlement sites in Albay, Philippines were reviewed to test the proposed site
525 selection model parameters for settlement or resettlement sites as well as examined the actuality of

526 *Geophilosophical* realism of assessing the potential risk recurring in addition to the accumulated residual risk
527 from past hazard events.
528
529 Abante, A. M. R. designed the Hexagonal Binning technique to store the risk hotspot or coldspot information to
530 mimic the risk reality in Albay and developed the geospatial information data model to demonstrate that the
531 complexities in quantifying risk reality is doable.
532
533 Abante, A. M. R. devised the geophilosophical Metatheorem objects in her dissertation for the Doctor of Philosophy
534 in Development Management to prove the mathematical logic that demonstrates the risk realness varies at
535 different extents of stability. Her dissertation proved that risk trend is a calculated risk reality (risk hotspot) in
536 addition to the residual risk (ΔR) and Phi (φ) when risk exceeds 125-unit quantity.

537 **Acknowledgements**

538 The road to completing the dissertation was fraught with many obstacles and challenges that were overcome due
539 both to the persistence and motivation of its maker, and the support of all those who have given much more than
540 their time and minds. I dedicate this section to such extraordinary persons who have taken away much from them,
541 only to give more to others. The creation and refinement of knowledge is no small feat and can only be done with
542 the support of others. My adviser in this dissertation, Dr. Jose Leandro A. Lanuzo generously imparted his unique
543 perspectives and allegories on theories and concepts of development management. His insights greatly improved my
544 own views and understanding of the discipline that surround my work. His willingness to share his mind is a great
545 act of generosity that I am truly grateful for. A dissertation, however, is a complex work of art and skill that also
546 requires expertise in specific disciplines. I am fortunate to have had the guidance of my external panelists Dr.
547 Encarnacion N. Raralio, and her husband Dr. Pedro Raralio, for their sharing technical expertise to complete this
548 manuscript. Among them, I also extend my greatest thanks to Ms. Arlene E. Dayao, for her invaluable expertise in
549 geosciences. Dissertation Committees are often viewed as gates or hurdles to overcome, but in my case, I have been
550 graced by one which has often been the source of direction and motivation. Atty. Alex B. Nepomuceno as the
551 Chairperson, and the members: Atty. Joseph L. Bartolata, PhD, Dr. Benedicto B. Balilo, DIT, Ar.EnP. Encarnacion
552 N. Raralio, PhD. and Arlene E. Dayao, MSc. have my gratitude for their unceasing willingness to see me through
553 this achievement. Their wisdom was a torch that lit the way through a familiarly dark path. I also wish to
554 acknowledge the open-source data of NAMRIA, PhilGIS, Project NOAH, PhilLIDAR, DENR-MGB, DENR-MGB,
555 PHIVOLCS, and Open Street Maps and its contributors. The data they continue to provide are valuable sources of
556 information for researchers in my field. Also, the complex analyses conducted in this paper would have been
557 difficult to implement without the personal use license and access provided by the Environmental Science Research
558 Institute (ESRI). I am also dedicating this section to a few more people, who, in their own capacities as colleagues
559 and friends, have been instrumental to the completion of this work. Dr. Arnulfo M. Mascariñas, Bicol University
560 President; Dr. Helen M. Llenaresas, Vice-President for Academic Affairs; Engr. Amelia B. Gonzales, PhD,
561 BUCENG Dean; Dr. Noemi L. Ibo, JMRIGD Director; and Dr. Antonio P. Payonga, BU Graduate School Dean.
562 They work tirelessly to transform the University into a world-class university. Engr. Teodora Bandojo from the
563 National Housing Authority has my great thanks for providing the data on NHA resettlement sites. Other forms of
564 support and assistance also helped me in this endeavor: my son EnP. Carlo Gabriel R. Abante for his technical
565 support; my student Louie Jennidene V. Ramirez for her drawings and illustrations; and my eldest son Paolo Gabriel
566 for accompanying me during my site visits. Their voluntary efforts are greatly appreciated. To all my classmates in
567 the Development Management program, thank you for the encouragement to complete this work; To all my friends
568 who stayed by my side during all the difficult times, thank you for the friendship; To my mother Heidi L. Rico,
569 thank you for your persistence to motivate me to finish my doctoral degree; To my children Paolo, Carlo, Marco,
570 and Marietoni, thank you for your unconditional love; I dedicate this manuscript to my late husband Anthony, who
571 was my silent confidant and critic. His openness and patience never wavered, despite his Parkinson's Disease. Until
572 his very end, he remained my closest adviser. Above all, I dedicate this dissertation to The Almighty God, the source
573 of all that I have. May my work and my achievements in life always serve the benefit of his creation.

574 **Authors' information**

575 The author completed Doctor of Philosophy in Development Management at the Jesse M. Robredo Institute, Bicol
576 University in July 4, 2020; a holder of Professional Masters in Geoinformatics with Specialization in Development
577 and Maintenance of Geographic Information Systems, International Institute for Aerospace Surveys and Earth
578 Sciences (ITC), Enschede, The Netherlands; a recipient of Netherlands Fellowship Program (NFP) in 1997; a
579 graduate of Applied Geodesy and Photogrammetry, University of the Philippines, Training Center for Applied
580 Geodesy and Photogrammetry in 1992; and a graduate of Bachelors of Science in Civil Engineering, Bicol
581 University College of Engineering, Legazpi City in 1989. Presently connected as a faculty in BU College of
582 Engineering. She authors researches that focus in applying geoinformatics in environmental planning and disaster
583 risk reduction. She published four papers in 2018-2019. She received 2 best paper in Bicol University in 2018-2019
584 and recently attended various training on basic meteorology, flood risk modeling, Safe and Resilient Cities,
585 geomatics and planning, remote sensing, unmanned aerial vehicle road mapping, space science and technology, etc.
586 The author is licensed to practice environmental planning, geodetic engineering and civil engineering in the
587 Philippines.

588 **References**

- 589 ¹ Abante, A. M. R. (2020). Unpublished Dissertation entitled “Geophilosophical Perspective on Socio-spatial Fuzzy
590 Reality Phenomenon”. Bicol University, Legazpi City Philippines
- 591 ² Pellini, A., Jabar, M., Era, M., & Erasga, D. (2013). Towards policy-relevant science and scientifically informed
592 policy: Political economy of the use of knowledge and research evidence.
- 593 ³ Gerona, D. M. (2013). Guinobatan
- 594 ⁴ Abante, A. M. R., & Balilo Jr, B. B. (December 2018). Resource Location-Intelligence Model Conceptualized for
595 Mayon Volcano Danger Zones in Albay, Philippines. *International Journal of Computing Sciences*
596 *Research*, 2(2), 55-67.
- 597 ⁵ Gärdenfors, P. (2004). *Conceptual spaces: The geometry of thought*. MIT press.
- 598 ⁶ Abante, A. M. R. (December 2018). Understanding Preparedness Insufficiency in the Context of DRRM: A Case
599 Study in Malinao, Albay, Philippines. In *Recent Advances in Geo-Environmental Engineering,*
600 *Geomechanics and Geotechnics, and Geohazards* (pp. 497-501). Springer, Cham.
- 601 ⁷ Woodard, B. (2013). *On an ungrounded earth: Towards a new geophilosophy*. punctum books.
- 602 ⁸ Woodward, K. (2016). Geophilosophy. *International Encyclopedia of Geography: People, the Earth, Environment*
603 *and Technology: People, the Earth, Environment and Technology*, 1-8.
- 604 ⁹ Abante, A. M. R. & Abante, C. G. R. (December 2019). TOPOPHILIA-EXPOSURE CENTRAL SPACE
605 CONCEPT MODEL, *Int. Arch. Photogramm. Remote Sens. Spatial Inf. Sci.*, XLII-4/W19, 1–8,
- 606 ¹⁰ Abante, A. M. R., & Abante, C. G. R. (2018, February). Sensitive Land Use Planning, Malinao, Albay,
607 Philippines. In *IOP Conference Series: Earth and Environmental Science* (Vol. 123, No. 1, p. 012001). IOP
608 Publishing
- 609 ¹¹ Birkmann, J. (2006). Measuring vulnerability to promote disaster-resilient societies: Conceptual frameworks and
610 definitions. *Measuring vulnerability to natural hazards: Towards disaster resilient societies*, 1, 9-54.
- 611 ¹² Birkmann, J., & Wisner, B. (2006). Measuring the unmeasurable: the challenge of vulnerability. *UNU-EHS*.
- 612 ¹³ King, L. J. (2020). Central place theory.
- 613 ¹⁴ Scott, L. M., & Janikas, M. V. (2010). Spatial statistics in ArcGIS. In *Handbook of applied spatial analysis* (pp.
614 27-41). Springer, Berlin, Heidelberg.
- 615 ¹⁵ Worboys, M. F., & Duckham, M. (2004). *GIS: a computing perspective*. CRC press.
- 616 ¹⁶ Rolf, A., & de By, R. A. (2000). *Principles of geographic information systems*. The International Institute for
617 *Aerospace Survey and Earth Sciences (ITC), Hengelosestraat, 99.*
- 618 ¹⁷ Getis, A., & Getis, J. (1966). Christaller's central place theory. *Journal of Geography*, 65(5), 220-226.
- 619 ¹⁸ Ord, J. K., & Getis, A. (1995). Local spatial autocorrelation statistics: distributional issues and an
620 application. *Geographical analysis*, 27(4), 286-306.
- 621 ¹⁹ Pearson, L., & Pelling, M. (2015). The UN Sendai framework for disaster risk reduction 2015–2030: Negotiation
622 process and prospects for science and practice. *Journal of Extreme Events*, 2(01), 1571001.
- 623 ²⁰ Quito Declaration on Sustainable Cities and Human Settlements for All.

- 624 ²¹ IPCC Second Assessment Report WGIII - Climate Change 1995: Economic and Social Dimensions of Climate
625 Change
- 626 ²² National Disaster Risk Reduction and Management Plan (NDRRMP) 2011- 2028
- 627 ²³ Flood Forecasting and Flood Hazard Mapping for Bicol River Basin, Disaster Risk Exposure and Assessment for
628 Mitigation (DREAM), DOST Grants in-Aid Program, 61 pp.
- 629 ²⁴ Joint DENR-DILG-DND-DPWH-DOST Adoption of Hazard Zone Classification on (2014)
- 630 ²⁵ Assessment of Disaster Risk Reduction and Management (DRRM) at the Local Level. Commission on Audit
631 (2014)
- 632 ²⁶ Daep, C. D. (2011) Bicol University Graduate School Unpublished Dissertation entitled “The Implementation of
633 the Disaster Risk Reduction Management Program in the Province of Albay”. Bicol University Dissertation.
- 634 ²⁷ Hofmann, M. (2007). Resilience. A formal approach to an ambiguous concept (Doctoral dissertation,
635 Diplomarbeit, Fachbereich für Mathematik und Informatik, Freie Universität Berlin).
- 636 ²⁸ Couclelis, H. (2005). “Where has the future gone?” Rethinking the role of integrated land-use models in spatial
637 planning. *Environment and planning A*, 37(8), 1353-1371.
- 638 ²⁹ Gregory, D., Johnston, R., Pratt, G., Watts, M., & Whatmore, S. (Eds.). (2011). *The dictionary of human
639 geography*. John Wiley & Sons.
- 640 ³⁰ Hadjimichalis, C. (2011). Uneven geographical development and socio-spatial justice and solidarity: European
641 regions after the 2009 financial crisis. *European Urban and Regional Studies*, 18(3), 254-274.
- 642 ³¹ Situational Report No.57 re Mayon Volcano Eruption - ndrrmc.
- 643 ³² Aubrecht, C., Özceylan, D., Steinnocher, K., & Freire, S. (2013). Multi-level geospatial modeling of human
644 exposure patterns and vulnerability indicators. *Natural Hazards*, 68(1), 147-163.
- 645 ³³ Carreño, M. L., Cardona, O. D., & Barbat, A. H. (2007). A disaster risk management performance index. *Natural
646 Hazards*, 41(1), 1-20.
- 647 ³⁴ Gregory, D. (1989). Areal differentiation and post-modern human geography. In *Horizons in human
648 geography* (pp. 67-96). Palgrave, London.
- 649 ³⁵ Birkmann, J., & Wisner, B. (2006). Measuring the unmeasurable: the challenge of vulnerability. *UNU-EHS*.
- 650 ³⁶ Cutter, S. L., Boruff, B. J., & Shirley, W. L. (2003). Social vulnerability to environmental hazards. *Social science
651 quarterly*, 84(2), 242-261.
- 652 ³⁷⁶ Cutter, S. L. (2003). The vulnerability of science and the science of vulnerability. *Annals of the Association of
653 American Geographers*, 93(1), 1-12.
- 654 ³⁸ Cutter, S. L., Boruff, B. J., & Shirley, W. L. (2003). Social vulnerability.
- 655 ³⁹ Birkmann, J., Cardona, O. D., Carreño, M. L., Barbat, A. H., Pelling, M., Schneiderbauer, S., ... & Welle, T.
656 (2013). Framing vulnerability, risk and societal responses: the MOVE framework. *Natural hazards*, 67(2),
657 193-211.
- 658 ⁴⁰ Cardona, O. D., van Aalst, M. K., Birkmann, J., Fordham, M., McGregor, G., & Mechler, R. (2012). Determinants
659 of risk: exposure and vulnerability.
- 660 ⁴¹ Cuevas, S. C., Peterson, A., Robinson, C., & Morrison, T. H. (2016). Institutional capacity for long-term climate
661 change adaptation: evidence from land use planning in Albay, Philippines. *Regional environmental
662 change*, 16(7), 2045-2058.
- 663 ⁴² Salceda, J. S. (2012). Adapting to climate change: Strategies of Albay, Philippines. *Agriculture and Development
664 Notes on Climate Change Adaptation*, 2.
- 665 ⁴³ Resilience in Albay, Philippines. *Climate Change Adaptation and Disaster Risk Reduction: An Asian Perspective*,
666 237-259.
- 667 ⁴⁴ Andam Lahar: Anticipation Action for Lahar Risks Preparedness Module for Rain Induced Lahar.
- 668 ⁴⁵ Contreras, D., Blaschke, T., & Hodgson, M. E. (2017). Lack of spatial resilience in a recovery process: Case
669 L'Aquila, Italy. *Technological forecasting and social change*, 121, 76-88.
- 670 ⁴⁶ Dikeç, M. (2001). Justice and the spatial imagination. *Environment and planning A*, 33(10), 1785-1805.
- 671 ⁴⁷ Dupont, V. (2004). Socio-spatial differentiation and residential segregation in Delhi: a question of
672 scale? *Geoforum*, 35(2), 157-175.
- 673 ⁴⁸ International Forum for Social Development Social Justice in an Open World The Role of the United Nations.

Figures

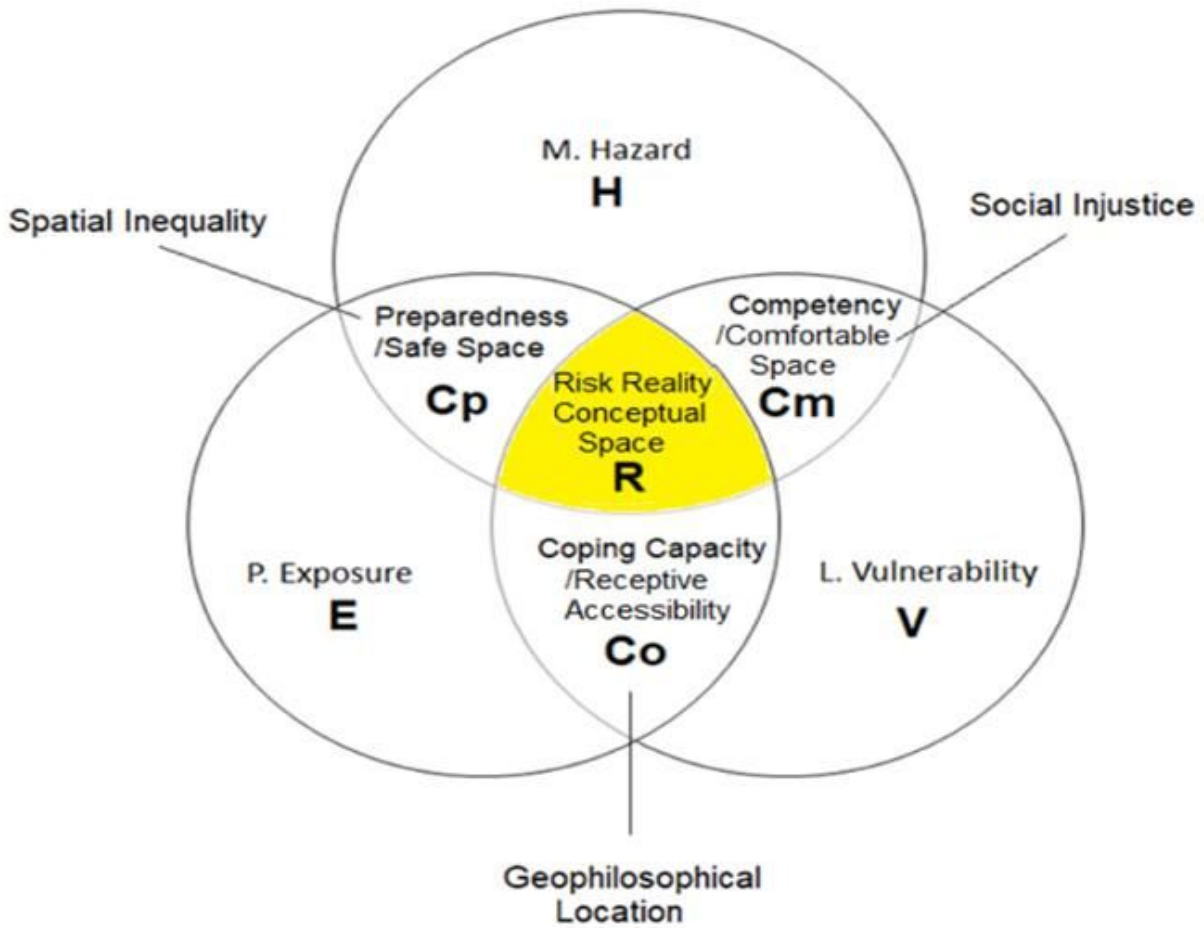


Figure 1

Risk Reality Conceptual Space (Abante, 2020)

Risk Reality		Class	Very High Risk	High Risk	Moderate	Low Risk	Very Low Risk
Description			95 to 99% Hotspot	90 to 95% Hotspot	Neutral	90 to 95% Coldspot	95 to 99% Coldspot
Risk Element	Multiple Hazards	Quantity	≥ 500	≥ 450 < 500	≥ 180 < 450	≥ 60 < 180	< 60
		Description	Very High Multiple Hazards	High	Moderate	Low	Very Low
	Landscape Vulnerability	Quantity	≥ 13	≥ 10 < 13	≥ 8 < 10	≥ 5 < 8	< 5
		Description	Critical Condition	Somewhat Unsafe Condition	Neutral	Somewhat Safe	Stable Space
	Passive Exposure	Quantity	5	4	3	2	1
		Description	Critical location	Unsafe location	Neutral	Somewhat Safe Location	Safe Location
	Preparedness	Quantity	5	4	3	2	1
	Description	Unprepared	Insufficient Preparedness	Neutral	Somewhat Prepared	Prepared	
Competency	Quantity	5	4	3	2	1	
	Description	Incompetent	Somewhat Incompetent	Neutral	Somewhat Competent	Competent	
Coping Capacity	Quantity	5	4	3	2	1	
	Description	In bad condition	Poor Coping Capacity	Neutral	Somewhat High Coping Capacity	High Coping Capacity	

Figure 2

Risk Reality Binning Parameters (Abante, 2020)

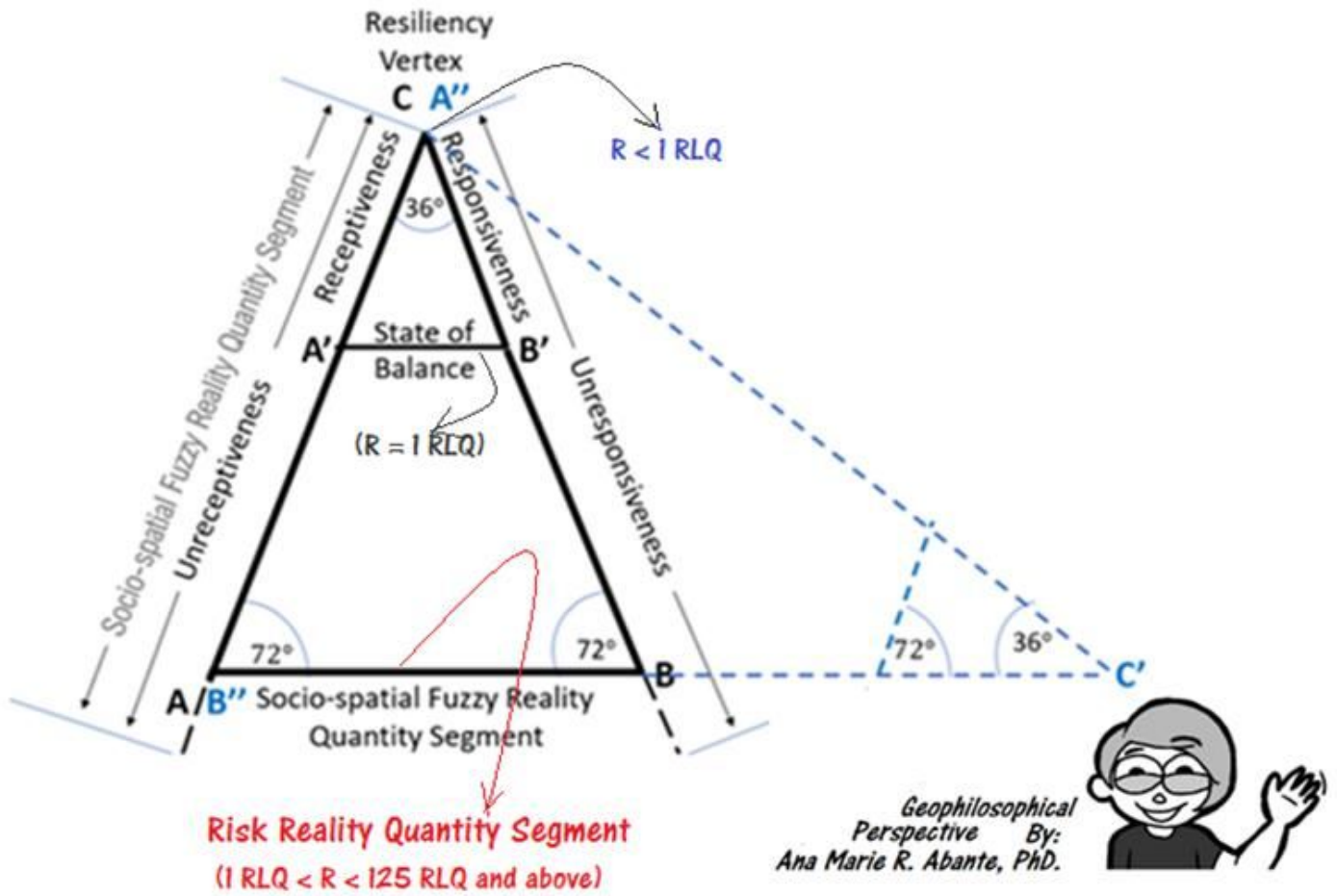


Figure 3

Risk Reality Isosceles Δ Grounded by Schoen Δ (Abante, 2020)

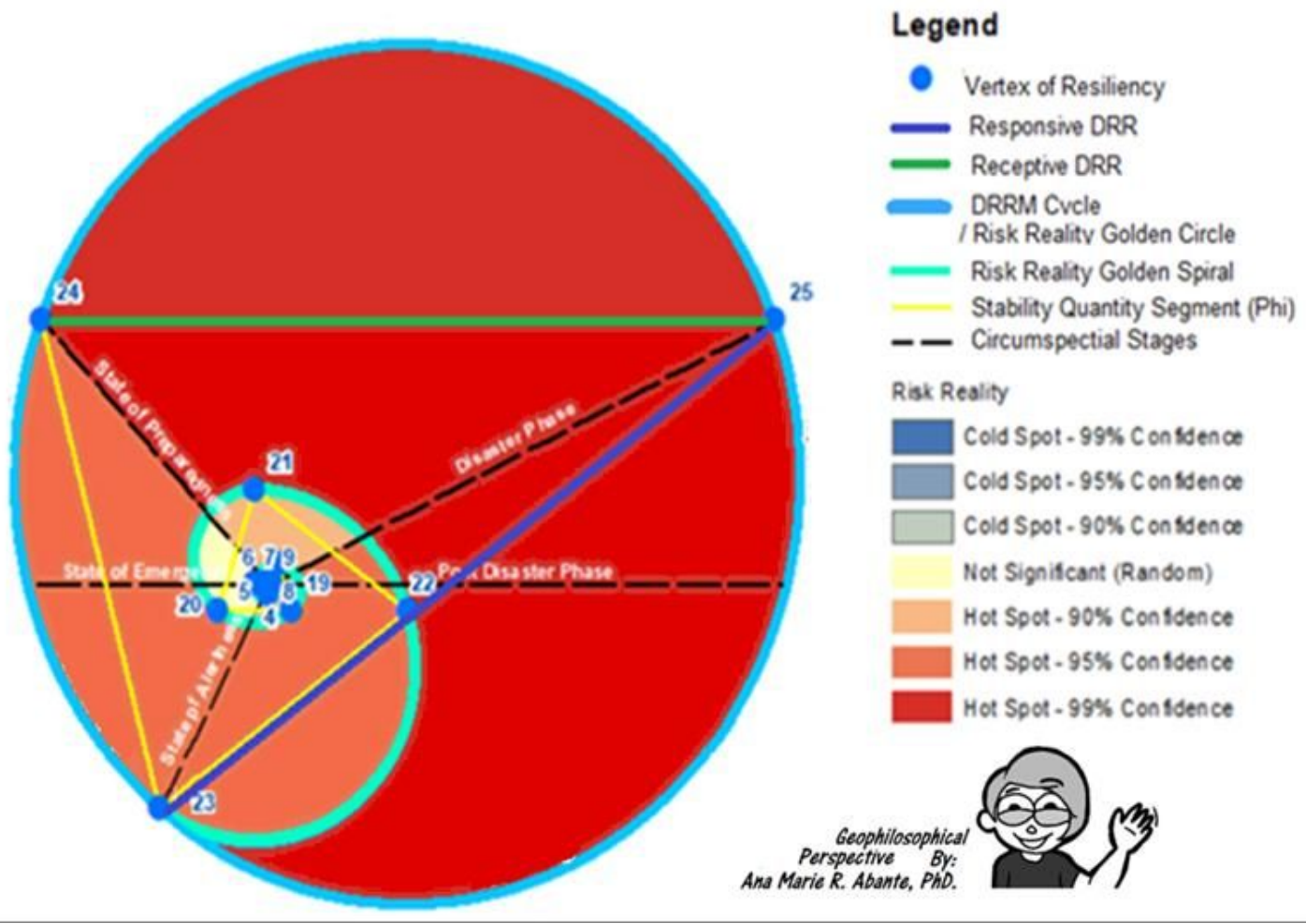


Figure 4

Risk Reality Circle Grounded by Fibonacci Golden Ratio and Schoen Golden Triangle (Abante, 2020)

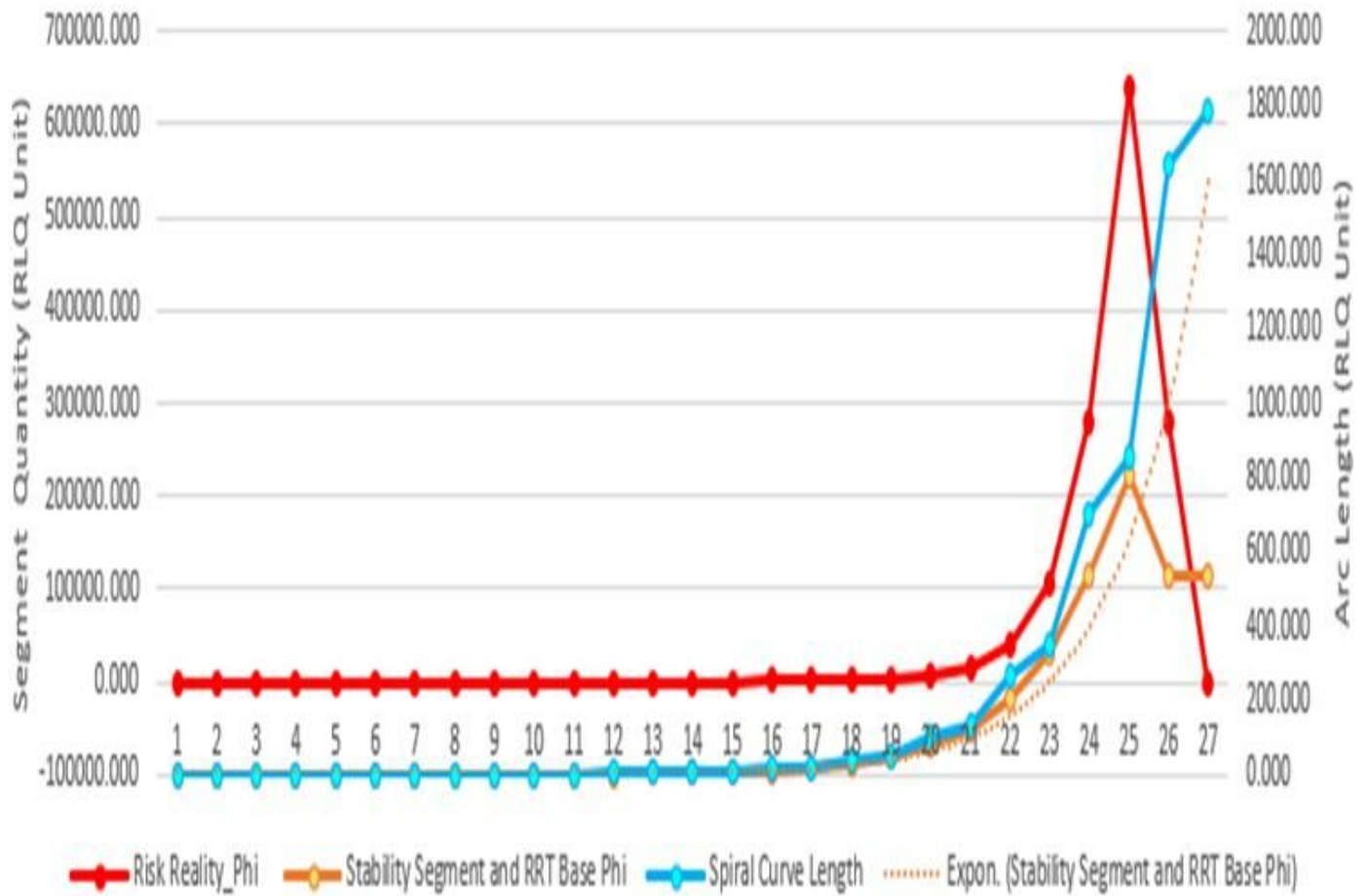


Figure 5

Risk Reality Quantity Chart (Abante, 2020)

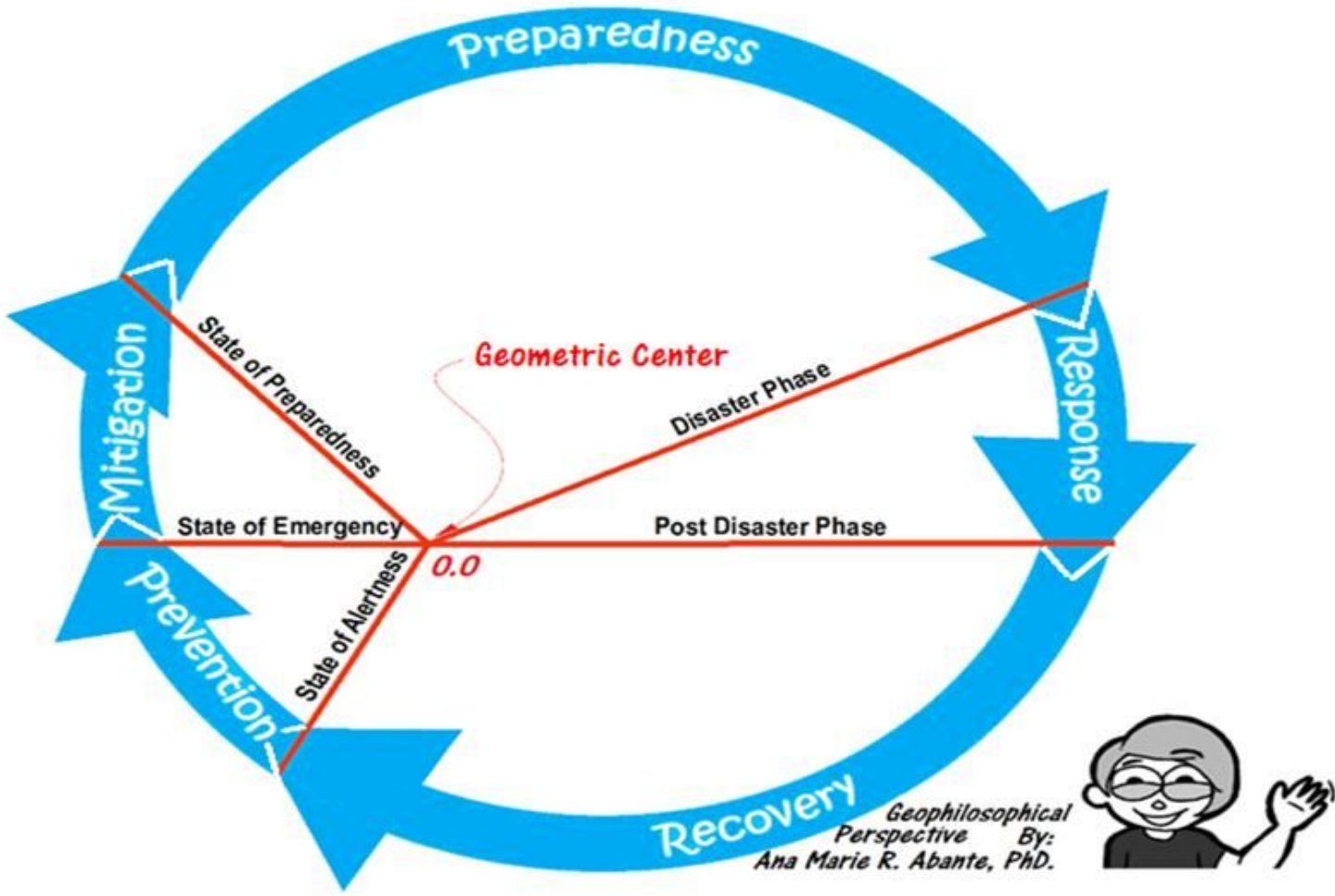


Figure 6

DRRM-Circumspectal Isometric Stages Parameter (Abante, 2020)

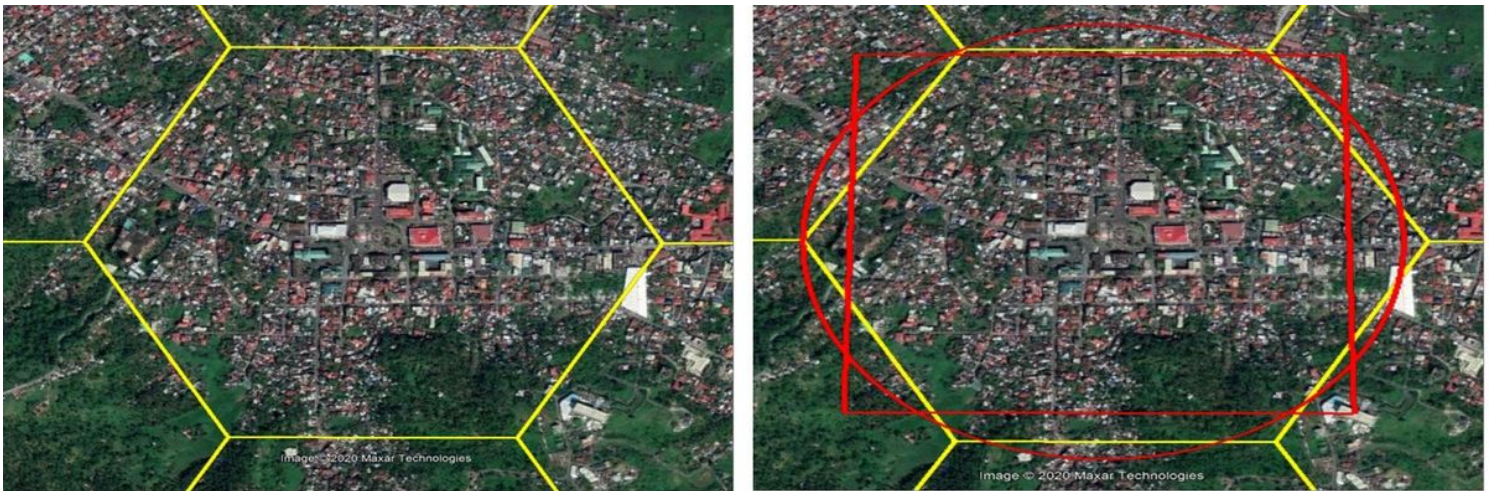


Figure 7

Tessellated Hexagonal Bins (Polygons)

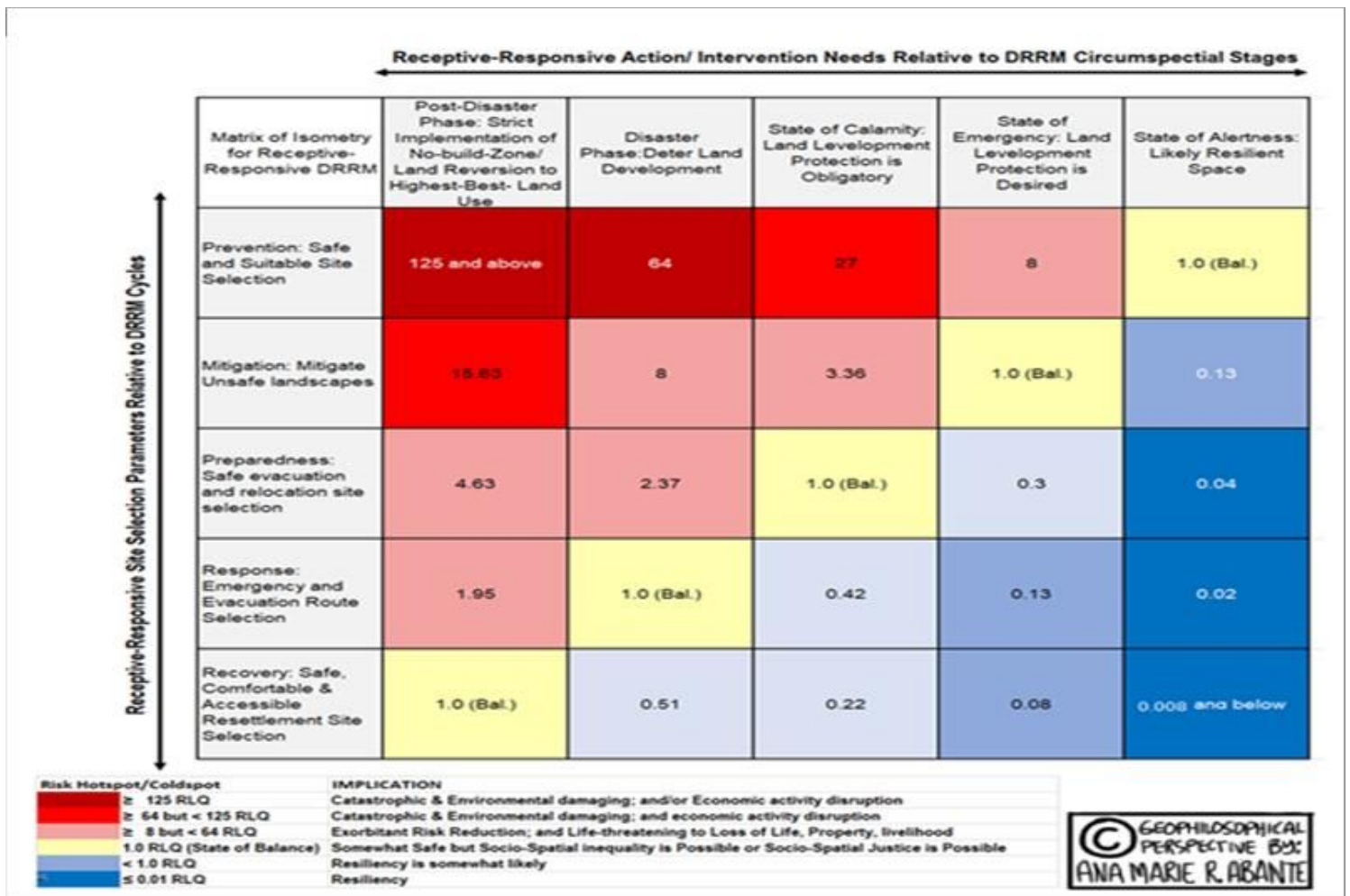
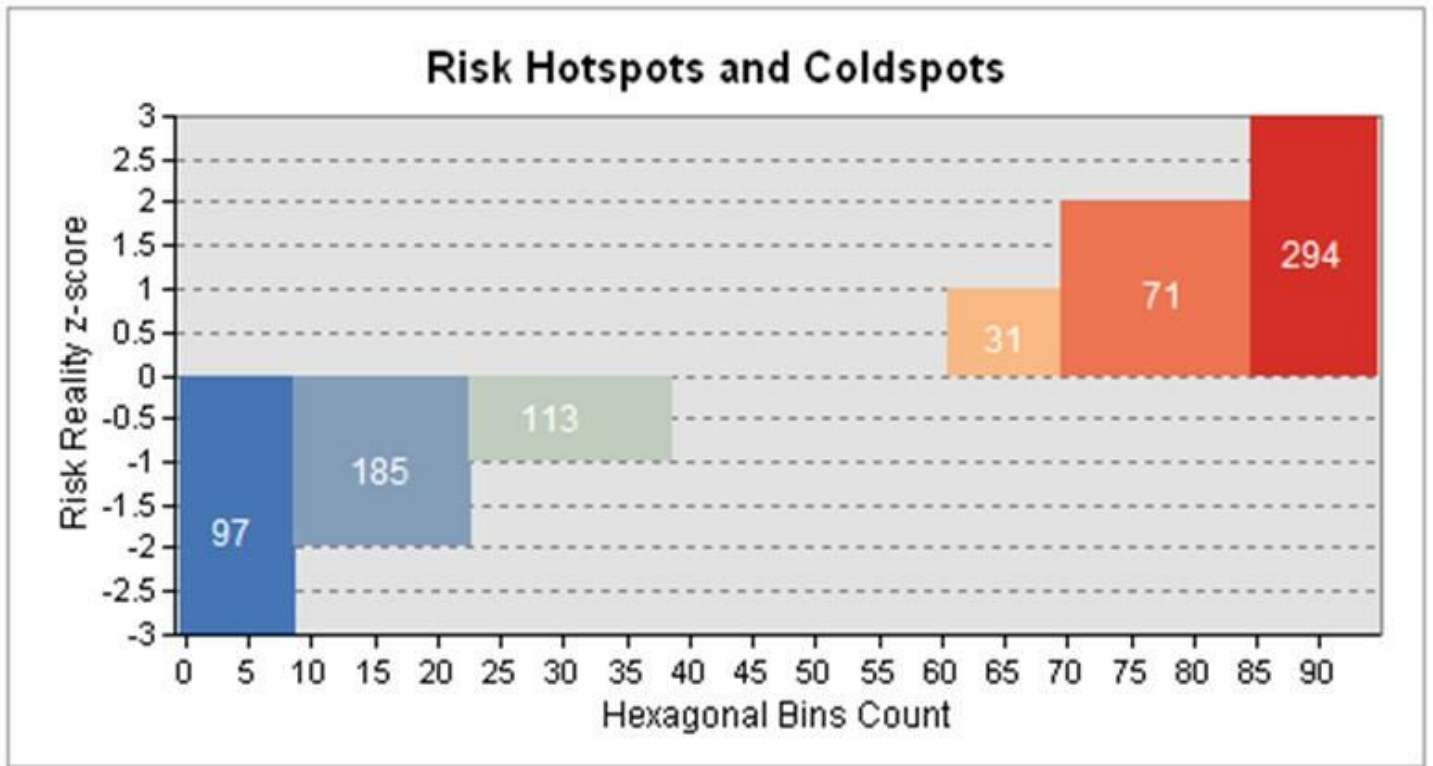


Figure 8

Receptive-Responsive DRR Isometric Index (Abante, 2020)



- Cold Spot - 99% Confidence
- Cold Spot - 95% Confidence
- Cold Spot - 90% Confidence
- Not Significant
- Hot Spot - 90% Confidence
- Hot Spot - 95% Confidence
- Hot Spot - 99% Confidence

Figure 9

Risk Hotspots and Coldspots Bin Count

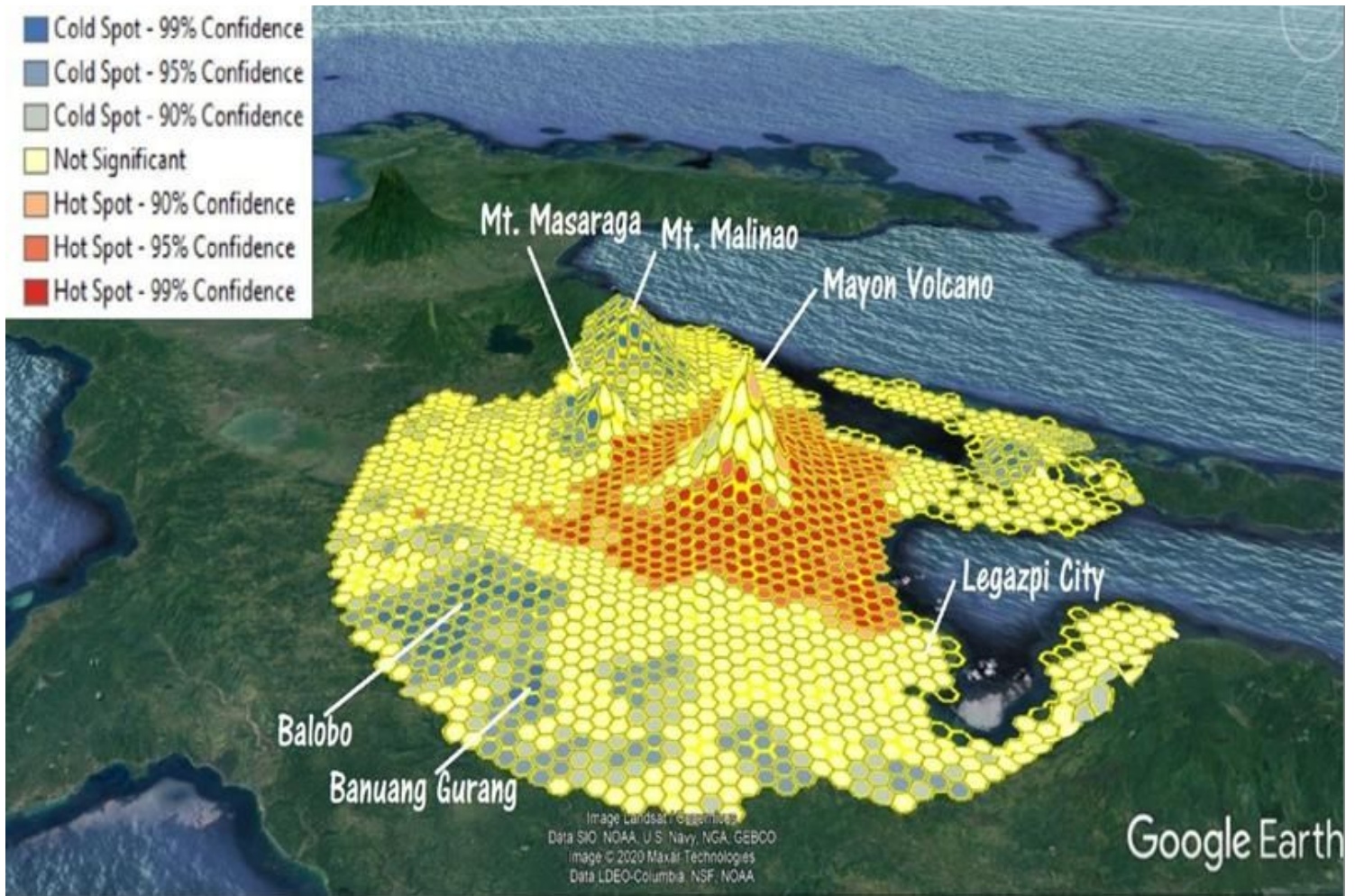


Figure 10

Risk Hotspot and Coldspot Tessellated Bins Visualization in Google Earth Platform

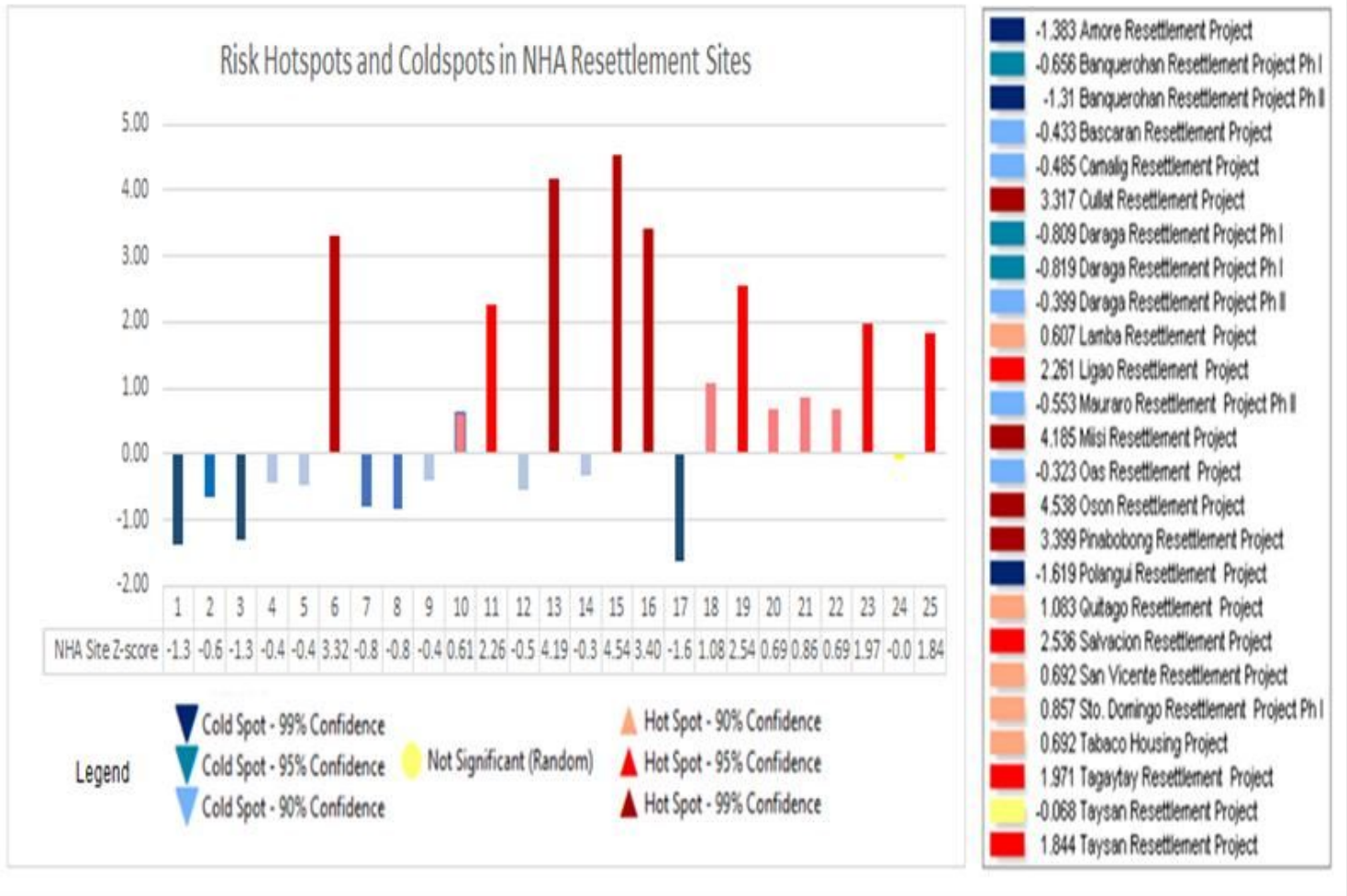


Figure 11

Risk Realness in Resettlement Sites in Albay, Philippines

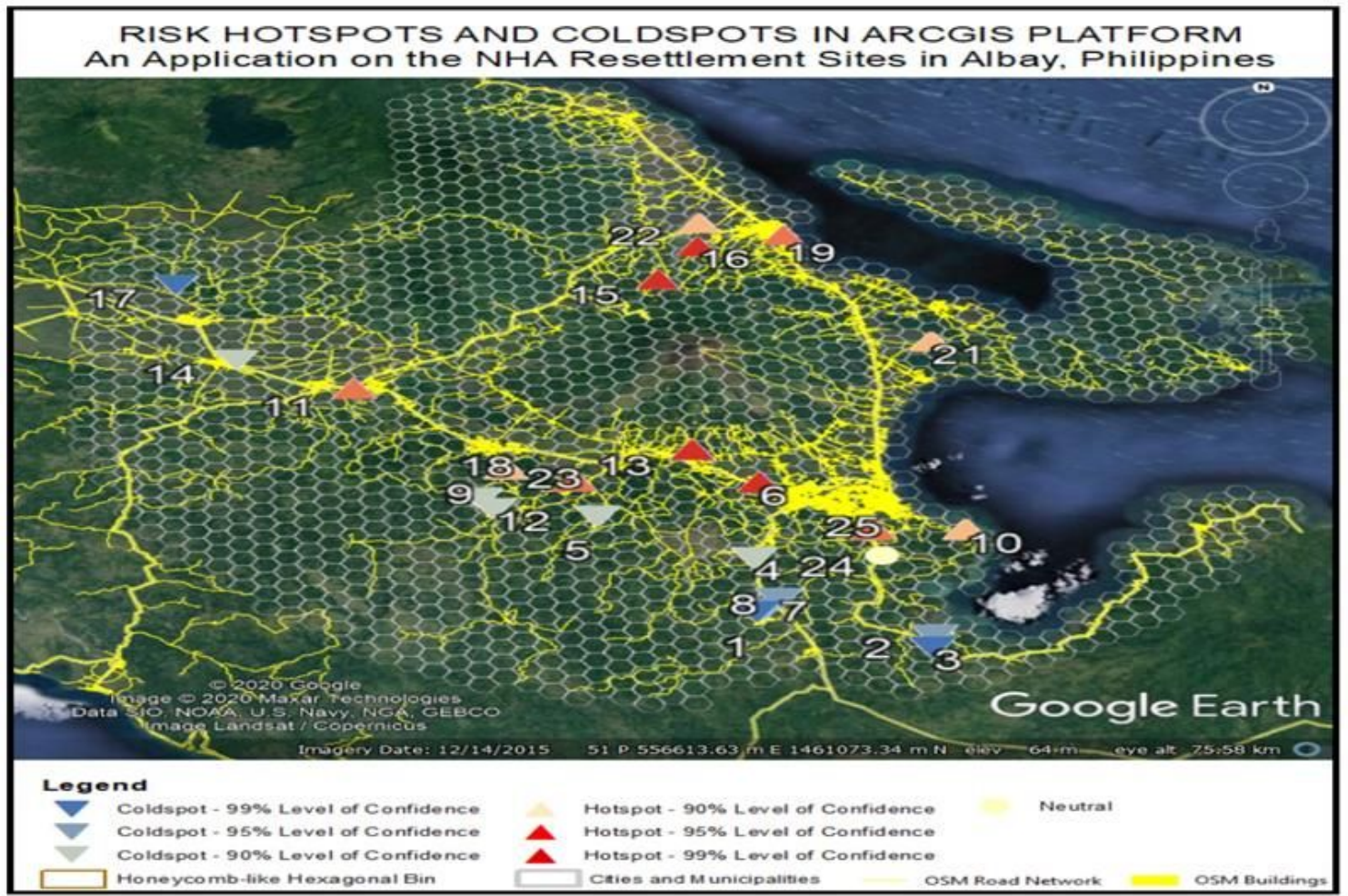


Figure 12

Risk Reality in NHA Resettlement Sites in Albay, Philippines